

**NACA**

# RESEARCH MEMORANDUM

MAGNESIUM-SLURRY COMBUSTION PERFORMANCE IN  
6.5-INCH-DIAMETER RAM-JET ENGINE MOUNTED  
IN CONNECTED-PIPE FACILITY

By J. Robert Branstetter, James B. Gibbs  
and Warner B. Kaufman

Lewis Flight Propulsion Laboratory  
Cleveland, Ohio

Classification: no 1-0 (or changed to *Unclassified*)  
By: *Nasa Tech Pub Announcement #116*  
By: *5 July 57*  
*OK*

GRADE OF OFFICER MAKING CHANGE)

*31 Mar 61*

**NATIONAL ADVISORY COMMITTEE  
FOR AERONAUTICS**

WASHINGTON  
August 5, 1953

NACA RM E53E27

6821

0143401

TECH LIBRARY KAFB, NM



0143401

1V

NACA RM E53E27

~~CONFIDENTIAL~~

## NATIONAL ADVISORY COMMITTEE FOR AERONAUTICS

RESEARCH MEMORANDUM

## MAGNESIUM-SLURRY COMBUSTION PERFORMANCE IN 6.5-INCH-DIAMETER

## RAM-JET ENGINE MOUNTED IN CONNECTED-PIPE FACILITY

By J. Robert Branstetter, James B. Gibbs, and Warner B. Kaufman

## SUMMARY

The performance of slurry fuels consisting of 50 percent magnesium powder in a hydrocarbon carrier was investigated in a flight-type, 6.5-inch-diameter ram-jet engine mounted in a connected-pipe facility. A combustor configuration was developed that provides acceptable combustion performance for equivalence ratios between 0.39 and 0.95. Combustion limits were not determined. At the richest equivalence ratio investigated, 0.95, the air specific impulse was 178 seconds, the air specific impulse efficiency was 96 percent, and the combustor efficiency was 86 percent. At the aforementioned equivalence ratio and for a simulated free-stream Mach number of 2.3 and altitudes above the tropopause, the gross thrust coefficient was 1.29. Satisfactory ignition and starting characteristics were achieved over an equivalence ratio range of 0.65 to 0.90. All combustor parts successfully withstood a durability test of 78 seconds duration. Only a thin layer of magnesium oxide was deposited on the combustor parts and nozzle.

Performance comparisons were made between the developed slurry system and the data obtained in the free-jet and flight tests of similar ethylene-fueled ram-jet engines at the NACA Langley laboratory. The thrust coefficients provided by the slurry fuel were greater than those of the ethylene system for equivalence ratios greater than 0.4. The maximum net thrust coefficient for the slurry was 1.43 times the maximum obtained with the ethylene at a simulated free-stream Mach number of 2.3 and altitudes above the tropopause. The slurry-fueled ram-jet engine produced considerably higher fuel volume specific impulse; however, the fuel weight specific impulse was slightly higher for the ethylene system. At constant air flow and comparable gross thrust coefficients, the combustion-chamber-inlet pressure generally was lower for the slurry than for the ethylene fuel. The slurry combustor-fuel combination appears suitable for flight testing and should provide appreciable increases in maximum velocity, acceleration, and range over those obtained with the ethylene-fueled vehicle.

~~CONFIDENTIAL~~~~Handwritten signature~~

2755

1-10

## INTRODUCTION

The combustion performance of metal slurry fuels, that is, metal powders suspended in liquid hydrocarbons, has been investigated in small-scale, jet-engine-type apparatus (refs. 1 and 2). The investigations indicate that it is possible to achieve greater thrust and wider combustion limits with magnesium slurries than with petroleum fuels. Because of these performance characteristics, magnesium slurries appear to be well suited for applications to jet engines such as the ram-jet engines used for powering short-range vehicles. A vehicle of this type is being employed at the NACA Langley Laboratory to obtain supersonic aerodynamic data. The vehicle has many desirable flight characteristics provided good combustion performance can be achieved in the two short, 6.5-inch-diameter ram-jet engines installed in the tail surfaces (ref. 3). Ethylene, a high-flame-speed gaseous fuel, has been used to achieve acceptable combustion in the short combustors (refs. 4, 5, and 6). The favorable thermodynamic properties reported in reference 7 and the good combustion performance reported in references 1 and 2 indicate that gains in performance may be expected in application of magnesium slurry fuel to the vehicle. Consequently, a cooperative research project between the NACA Lewis and Langley laboratories was established wherein the Lewis laboratory undertook the development of a combustor for the flight-type engine that would use magnesium slurry fuel.

For the program reported herein, a slurry composition of 50 percent magnesium powder and 50 percent hydrocarbon fuel by weight was selected; this selection was based on the data of references 1, 2, and 7 and an investigation of the physical characteristics of slurries (ref. 8). The slurry fuel was evaluated in a 6.5-inch-diameter flight-type engine which was mounted in a connected-pipe facility. The tests encompassed a range of combustor-inlet conditions similar to those reported for a flight test of the same engine (ref. 6). The performance of three particle-size grades of magnesium powder and of several flame-holder and injector configurations is reported herein. Data for the best performing slurry-engine configuration and a direct comparison between these data and ethylene performance (refs. 4 and 6) are discussed in detail. In addition, this investigation treats some of the pertinent physical problems encountered with slurry fuels.

## SYMBOLS

The following symbols are used in this report:

- A cross sectional area, sq in.
- B barrel thrust, lb

$C_N$	net thrust coefficient
$C_T$	gross thrust coefficient
$F$	total stream momentum at nozzle exit, lb
$g$	acceleration due to gravity, 32.17 ft/sec <sup>2</sup>
$M$	Mach number
$m$	mass flow rate, slugs/sec
$P$	total pressure, lb/sq in. abs
$p$	static pressure, lb/sq in. abs
$q$	kinetic pressure, lb/sq in.
$R$	gas constant for air, 53.3 ft-lb/(lb)(°R)
$S_a$	air specific impulse for sonic flow of exhaust products at nozzle throat, sec
$S_{f,vol}$	fuel volume specific impulse, lb-sec/cu ft
$S_{f,wt}$	fuel weight specific impulse, sec
$t$	static temperature, °R
$V$	velocity, ft/sec
$W$	weight flow rate, lb/sec
$\rho$	density, lb/cu ft
$\gamma$	ratio of specific heats
$\Phi$	equivalence ratio
$\varphi(M)$	stream momentum of jet expanded to the area of station 8 divided by stream momentum at station 9
Subscripts:	
0	inlet plenum
3	diffuser-inlet minimum area

- 7 diffuser exit
- 8 combustor exit
- 9 nozzle exit
- 12 exit plenum
- a air
- c denotes isentropic diffusion of air from station 7 to the maximum combustor area
- f fuel

#### FUEL AND APPARATUS

Fuel. - The fuel contained equal parts, by weight, of magnesium powder and a hydrocarbon fuel plus stabilizing additive. The powder particles were spherical in shape and were found by analysis to contain 98 percent free magnesium. Powders of three grades of fineness were used and, for the purposes of this report, were designated grades A, B, and C.

Grade	Amount passing 325-mesh screen, percent	Mean particle size, microns
A	60	30 - 40
B	95	17 - 23
C	100	3.5 - 5.0

The mean particle size was obtained with a Fisher Sub-Seive Sizer. An analysis of the hydrocarbon carrier, MIL-F-5624A grade JP-3 fuel, is given in table I.

The slurries were prepared in batches of 100 to 200 pounds each. Gelling or stabilizing agents, in quantities of 1/2 to 1 percent of the total mixture, were added to control viscosity. Methods of determining physical properties and the terminology describing the physical characteristics of metal-hydrocarbon slurries are presented in reference 8. During the first phase of the investigation, the fuel viscosity was particularly difficult to control; consequently, the fluidity and the stability of the slurry varied considerably from batch to batch. The

powder grade, slurry viscosity, and stability time for each batch are presented in table II. The density of the slurries was 1.05 grams per cubic centimeter and the lower heat of combustion was 14,770 Btu per pound. The stoichiometric fuel-air ratio was 0.1128.

Fuel system. - A schematic diagram of the basic fuel system used for the combustion tests is shown on figure 1. The fuel was supplied to the engine by pressurizing a 4-cubic-foot fuel tank with nitrogen. The rate of fuel flow was governed by the area of a flow-restricting orifice located upstream of the fuel injectors and by the controlled fuel tank pressure. The nominal diameter of the fuel feed line was  $1/2$  inch. The maximum fuel injection pressure was 600 pounds per square inch.

Ram-jet installation. - The engine was mounted as shown in figure 2. A 3-foot-long shroud was mounted on the diffuser lip in an effort to obtain a flat velocity profile at the entrance to the diffuser. A photograph of the installation with the inlet shroud removed is presented on figure 3. The inlet plenum and outlet plenum ducts were connected to the laboratory air supply and the atmospheric exhaust system, respectively. The combustion air, after passing through a tube-type heat exchanger, was metered and then throttled by a remotely controlled butterfly valve. The combustor shell was cooled by diverting a fixed portion (approximately 36 percent) of the combustion air through a  $1/2$ -inch annulus between the shell and a cooling jacket. The high external pressure impressed on the combustor by the cooling air necessitated the use of four longitudinal reinforcement bars and a combustor shell thickness of 0.093 inch. The cooling air recombined with the main portion of the combustion air in the inlet plenum and then entered the engine. A window in the inlet plenum permitted visual and photographic observation of the flame.

The combustion products were discharged into a barrel-type thrust target mounted in the exhaust plenum. The gases, after being cooled by water sprays located in the barrel and the vertical duct, passed through a fixed-baffle separator and into the exhaust stack.

Ram-jet engine. - A detailed description of the basic engine is presented in reference 6. A diagram of the engine, as modified for the present investigation, is shown in figure 4. The diffuser-lip diameter was 4.42 inches. The inside diameter and length of the Inconel combustor were  $6\frac{1}{2}$  and 19 inches, respectively. Convergent exhaust nozzles of 5.66- and 6-inch diameter were used.

The inner body of the basic engine of reference 6 was modified immediately downstream of the support struts to accommodate the slurry injector and the flame holder. A spring-loaded, variable-port-area injector, having four longitudinal slots spaced  $90^\circ$  apart, is shown in

figure 4. The piston area and the spring were designed to provide about 50 pounds per square inch pressure drop for the fuel-flow range investigated. An O-ring seal and silicone grease prevented seizing of the piston. Atomization of the fuel was achieved by impinging the fuel jets on a 4.5-inch-long cylindrical sleeve mounted in the air stream. The fuel slots were located 12 inches from the face of the flame holder (fig. 4). The flame holder was composed of V-gutters and funnels (surfaces of revolution of a cone) and blocked 46 percent of the combustor cross-sectional area. The material used for the flame holders was 1/16- or 3/32-inch-thick Inconel or stainless steel, or both. The aforementioned fuel injector and flame holder gave the best performance of the several types tested during the development program. This program is discussed in appendix A.

Ignition was provided by a magnesium flare of 8-inch length and 2-inch diameter with a nominal burning time of 45 seconds. The flare was cemented into a 1/16-inch-wall Inconel tube which fitted into the flame-holder cavity (fig. 4). The downstream (ignition) face of the flare and the downstream edge of the flame holder were located at the same axial station.

Instrumentation. - The combustion air flow was measured by a square-edged orifice conforming to A.S.M.E. standards. The portion of the combustion air temporarily diverted for cooling purposes was approximated by means of a pitot-static tube. The reaction of the thrust barrel to the force of the exhaust jet and the change in gross weight of the fuel tank were sensed by strain gages. Fuel-injection pressures were measured by a Bourdon gage located as shown in figure 1.

The inlet and exhaust plenum pressures, the combustion-air differential pressure, and the static pressures at stations 7 and 8 were sensed by Statham pressure pickups. These pressures and the two strain-gage forces were measured on an eight-channel oscillograph which recorded the data continuously as a function of time. The frequency response of the system was flat from 0 to 25 cycles per second.

Pressure pickups and self-balancing potentiometers recorded the following pressures at 2-second intervals:

- Combustion-air orifice differential pressure
- Combustion-air upstream orifice pressure
- Cooling-air static pressure
- Difference between cooling-air total and static pressure

Temperatures were measured with similar recording potentiometers at 12-second intervals at the following stations:

Combustion air, orifice  
Cooling air, inlet  
Cooling air, outlet (three parallel thermocouples)  
Combustion air, entering engine  
Fuel  
Combustor wall (four separate thermocouples)

#### PROCEDURE

The fuel flow rate and the thrust measuring apparatus were calibrated with dead weights prior to each run. The pressure-recording equipment was subjected to a comprehensive calibration approximately every 10 runs. An additional check of the instrumentation was made after each run by obtaining steady-state, cold-flow data at several air flows and comparing the recorded data to manometer and panel gage readings.

The slurry was thoroughly mixed on a barrel-roller immediately prior to testing. Some of the slurries listed in table II as "unstable" began to lose their homogeneity soon after the rolling ceased; however, the powder distribution in the carrier was believed to be reasonably uniform for the duration of the run. The slurry was transferred to the fuel tank by pressurizing the mixing barrel with nitrogen.

A small quantity of heated combustion air was passed through the apparatus before each run to permit the inlet air ducting to approach equilibrium temperature. Pressure was applied to the fuel tank and the recorder chart drives were turned on. The flare was ignited at low rates of air flow to reduce the danger of damage to the ignition leads. The air flow was rapidly increased to the starting condition and the fuel valve opened.

The fuel-tank pressure was held constant for 15 seconds or longer to provide sufficient time for determination of the fuel flow rate. During this period the air flow was varied over as wide a fuel-air ratio range as possible. If sufficient fuel remained and the flame was stable, the fuel flow was reduced and the procedure of varying the air flow was repeated. The duration of the tests seldom exceeded 2 minutes.

After the run, the fuel-tank system was drained and flushed with gasoline. The engine was disassembled and inspected for material failure and oxide deposits.

#### DATA REDUCTION

A sufficient number of data points were chosen from the records to define the performance over the range of fuel-air ratios investigated.



In order to reduce transient effects, points were selected when the air and fuel flow rates, thrust, and combustor pressures were either constant or changing only slowly with time.

The fuel flow rate was calculated from the slope of the fuel tank weight against time trace. Combustor-inlet velocity, Mach number, and kinetic pressure,  $V_c$ ,  $M_c$ , and  $q_c$ , respectively, were calculated assuming isentropic diffusion of air from station 7 to the maximum combustor area. Because of the area blockage afforded by the flame-holder case, the actual inlet velocities and Mach numbers were considerably higher than the values presented. Computations of the pressure at station 9, the exhaust nozzle, were made assuming isentropic, sonic flow of the exhaust products.

The usual parameters for expressing combustor performance based on temperature rise across the combustor are difficult to determine and are of questionable applicability for magnesium slurry fuels. This difficulty arises because the thermodynamic processes for heterogeneous solid-gas mixtures are not fully developed. It is advisable, therefore, to establish the performance of the fuels on the basis of parameters that account for the thermodynamic characteristics of the exhaust and are a measure of the thrust-producing capability. The parameters that appear most useful as an index of fuel performance are air specific impulse and fuel specific impulse (ref. 9). These impulse functions, which conveniently express the total stream momentum per pound of air and per unit of fuel referenced at the exhaust nozzle throat where the Mach number is equal to 1, are defined as:

Air specific impulse

$$S_a = \frac{F}{W_a} = \frac{p_9 A_9 + m V_9}{W_a}$$

where

$$m = \frac{W_a}{g} \left( 1 + \frac{W_f}{W_a} \right)$$

F for the experimental data equals

$$B + p_{12} A_9$$

The method for determining F is presented in appendix B.

Fuel weight specific impulse

$$S_{f,wt} = \frac{S_a}{W_f/W_a}$$

Fuel specific impulse is also determined on the volume basis, which indicates the volume rate of fuel consumption.

$$S_{f,vol} = (S_{f,wt}) \rho$$

The actual specific impulse data for the 50 percent magnesium slurries are compared to the theoretical values obtained from reference 7. The theoretical values were corrected to an inlet-air temperature of 350° F. Air specific impulse efficiency is then defined as

$$\left( \frac{S_{a,actual}}{S_{a,ideal}} \right) \times 100 \text{ at constant equivalence ratios}$$

Combustor efficiency for each datum point was determined by

$$\left( \frac{\phi_{ideal}}{\phi_{actual}} \right) \times 100 \text{ at constant } S_a$$

Gross thrust coefficients were computed for an engine in which the pertinent internal cross-sectional areas were the same as those given in reference 6.

$$C_T = \frac{AM \sqrt{\frac{\gamma g}{Rt}} \left[ S_a \phi(M) - \frac{M \sqrt{\gamma g R t}}{g} \right] - A_8}{\frac{\gamma}{2} M^2 A_8}$$

where

$$A = 0.1065 \text{ sq ft}$$

$$M = 2.3$$

$$t = 393^\circ \text{ R}$$

$$\gamma = 1.4$$

$$\phi(M) = 1.051 \text{ for } \gamma = 1.3$$

The combustor pressure losses were computed as a dimensionless ratio according to the following relation:

$$\frac{P_7 - P_8}{q_c}$$

where  $P_8$  was determined for a ratio of specific heats of 1.25.

## RESULTS AND DISCUSSION

## Slurry Performance

Engine performance. - This investigation was primarily directed toward the development of a slurry-fueled combustor for the flight vehicle. Therefore, the results discussed herein pertain to the development of an engine satisfactory for flight application. The requirements for the flight application were a combustor that would exhibit higher thrusts (air specific impulse) and more desirable fuel consumption than the ethylene combustor at the following conditions: inlet-air pressure, 30 to 60 pounds per square inch absolute; equivalence ratio, 0.5 to 0.9; inlet-air temperature, approximately 350° F; exit-nozzle throat diameter, 6.0 inches.

The engine development program, presented in appendix A, included an investigation of the effect of physical properties of magnesium slurries, fuel-injection variation, flame-holder configurations, exhaust-nozzle diameter, and ignition systems. The product of this program, a combustor which exhibited the best over-all performance, contained the following components: slurry, grade C (most reactive) powder in MIL-F-5624A grade JP-3 fuel; injector E, variable area with a 4.5-inch-long impingement surface; flame holder C, a gutter-funnel type, blocking 46 percent of the combustor-entrance area; exhaust nozzle, 6-inch-diameter throat; ignition device, a 2-inch-diameter, 8-inch-long magnesium flare. Table III presents the pertinent primary data obtained with this combustor-fuel combination. The precision of these data and the reliability of the results are presented in appendix B. The results that follow are for the aforementioned combustor-fuel combination.

Air specific impulse data. - Figure 5 presents air specific impulse as a function of equivalence ratio for the experimental and ideal performance of the slurry. Ideal octene-1 data, shown on the figure, were obtained from reference 7. Stable combustion was maintained over the range of equivalence ratios investigated from 0.39 to 0.95. At these equivalence ratios the experimentally determined impulse values were 118 seconds and 178 seconds, respectively. The corresponding ideal slurry impulse values were 137 and 185 seconds.

Effects of solid deposits. - During the early phases of this investigation, deposition of magnesium oxide and magnesium on the flame holder, combustor walls, and exit nozzle often resulted in excessive blockage of the flow area and excessive pressure drop across the engine (see appendix A). For the runs shown in table III and presented in figure 5, only a relatively thin coating of deposit was observed on the engine surfaces after each run. Combustor total-pressure-drop data (fig. 6) indicate the over-all pressure losses between stations 7 and 8. These pressure losses are presented as a function of density ratio across the combustor; the density ratio was computed from the approximated relation

$$\frac{\rho_c}{\rho_8} = \frac{p_c}{p_8} \frac{t_8}{t_c}$$

where  $t_8$  was estimated from the data of table III and reference 7. A solid line shown on the figure is the sum of the isothermal friction pressure losses obtained with a clean combustor and the idealized momentum pressure losses computed according to one-dimensional incompressible flow relations. These summed pressure losses were even greater than the measured losses which included the effect of solid deposits. Therefore, pressure losses due to solids adhering to the combustor surfaces were small with respect to the momentum and friction losses.

The effect of solids within the nozzle in reducing the nozzle area can be indicated by use of a one-dimensional flow relation. The total stream momentum at the exhaust nozzle can be expressed by the relation

$$F_9 = p_9 A_9' \left( 1 + \frac{\gamma M^2}{1 - \frac{W_{\text{solids}}}{W_{\text{total}}}} \right)$$

where  $A_9' = C_g A_9$ . Nozzle area blockage by solid deposits will affect the over-all area coefficient  $C_g$ . The nozzle was always choked and  $p_9$  was not measured; hence the equation may be rewritten as

$$F_9 = p_8 \frac{p_9}{p_8} C_g A_9 \left( 1 + \frac{\gamma}{1 - \frac{W_{\text{solids}}}{W_{\text{total}}}} \right)$$

The value  $p_9/p_8$  was computed by isentropic flow equations assuming that the area at station 9 was  $A_9'$  or  $C_g A_9$ .

The value of the area coefficient  $C_g$  prevailing in the combustion runs was found by comparing the experimentally determined variation of  $F_9$  against  $p_8$  with the variation computed from the previous equation using  $C_g$  of 0.9 and 1.0, as shown in figure 7. Since the equations are relatively insensitive to equivalence ratio and specific heat ratio, average values of 0.7 and 1.25, respectively, were used in the equation. All magnesium was assumed to be in the form of magnesium oxide. Figure 7 shows that the area coefficient of the experimental nozzle was 0.95, so that solid deposits could not have reduced the nozzle area by more than 5 percent. Furthermore, the constancy of the experimentally determined area coefficient would indicate that the maximum thickness of the oxide layer was attained within several seconds after initiation of combustion.

Effect of combustor-inlet velocity and pressure on performance. - The velocity and stagnation pressure at the combustor inlet and the air specific impulse are presented as a function of equivalence ratio with fuel flow rate as a parameter (fig. 8). Combustor velocities ranged from 220 to 340 feet per second at equivalence ratios of 0.9 and 0.4, respectively. For a given equivalence ratio, combustor-velocity deviations with change in fuel flow rate were about 5 percent from a mean value, and these deviations correlated with the change in impulse values. Combustor stagnation pressure ranged between 35 and 67 pounds per square inch absolute. Pressure and impulse data of figure 8 are cross-plotted on figure 9 for equivalence ratios of 0.45, 0.6, and 0.8. Within the limits of accuracy of the instrumentation and for the range of operating conditions investigated, combustor pressure had no effect on impulse performance.

Combustor and impulse efficiency. - Combustor efficiency and air specific impulse efficiency are presented on figure 10 as a function of equivalence ratio. These efficiencies were computed from the curves of air specific impulse against equivalence ratio (fig. 5). The mean value of combustor efficiency increased from a value of 66 percent at an equivalence ratio of 0.4 to 86 percent at 0.95 equivalence ratio. An impulse efficiency of 87 percent was obtained at an equivalence ratio of 0.4 and the efficiency increased to 96 percent at an equivalence ratio of 0.95.

The combustor-inlet velocity (fig. 8) progressively increased with decreasing equivalence ratio; consequently, the independent effect of either inlet velocity or equivalence ratio on combustor efficiency cannot be determined.

Heat transfer. - Experimental values of heat flux and combustor wall temperature obtained during run 97 are presented in figure 11. Although the air flow decreased somewhat as the run progressed (table III), the test conditions for this particular run were maintained as nearly constant as possible. Wall temperatures, 12.5 inches downstream of the flame holder, were less than 100° F higher than the cooling-air temperature. The flame zone apparently did not reach the combustor walls until it had traveled about 16 to 17 inches of the 19-inch-long combustor. The axial temperature gradient was 150° F per inch, 3 inches upstream of the nozzle entrance. Hence, the temperature gradient at the downstream station, which was 1.5 inches from the nozzle entrance, may have been of a similar magnitude. In all probability, combustor efficiency would be improved by an increase in combustor length; however, a longer combustor or more violent mixing of the burning products might require additional protective measures to prevent combustor wall burnout.

Since nearly all the radial heat flux was confined to a localized area, minor deviations in the location and seating of the flame could produce major deviation in the heat-transfer data.

Engine durability. - During run 87, the combustor pressure losses began to decrease 45 seconds after ignition as shown on figure 6. Photographs of the flame holder, taken before and after the run (fig. 12), show pronounced erosion of the cylindrical case and gutters. On the other four runs, the flame holder was only slightly damaged; however, the downstream end of the flare-holder case was usually burned away.

The flame holder used during run 97 was fabricated with one half of the funnels and gutters of Inconel and the other one half of 347 stainless steel. The thickness of these parts was increased from 1/16 to 3/32 inch. Although operating conditions were severe for a durability test, flame-holder damage was negligible for a run duration of 78 seconds. It was not possible to determine the better flame-holder material from this test. Durability for all combustor parts is believed to be adequate for short-range flight applications.

#### Comparison of Slurry and Ethylene Performance

Basis for comparisons. - The magnesium fuel performance was acceptable with regard to the range of stable combustion, air specific impulse values, freedom from solid deposits, combustor efficiency, ignition, durability of parts, and heat-transfer characteristics. The slurry performance data were next compared to the performance data of the ethylene-fueled ram-jet engine. The data for the ethylene performance (refs. 4 and 6) were obtained with the diffuser immersed in a supersonic air stream, which may have resulted in combustor-inlet velocity profiles different from those encountered in the present connected-pipe tests. Variations in velocity profile, by affecting the mixing of the fuel and air, could influence the combustion performance.

Comparison of thrust and fuel-consumption data. - Thrust and fuel consumption performance are presented on figures 13(a) and 13(b) for slurry and for ethylene fuels. The ideal and experimental slurry data and the ideal octene-1 data were obtained from figure 5. The ideal ethylene data were computed from adiabatic flame temperatures presented in reference 10. The experimental ethylene curves were computed from free-jet data reported in reference 4. The respective diffuser-entrance and nozzle-throat diameters for the latter tests were 3.95 and 5.75 inches, as compared to 4.42 and 6.0 for the slurry tests. Consequently, the combustor velocities associated with the ethylene data given on figure 13 were somewhat lower than those reported for the slurry tests. A flight test is reported (ref. 6) in which the diffuser and exit area dimensions were the same as those for the slurry data; however, the band of equivalence ratios was relatively small and a fuel system leak resulted in questionable accuracy of the fuel flow rate.

The fuel weight specific impulse is presented as a function of air specific impulse (fig. 13(a)). Over the range of air specific impulse obtained with ethylene, the fuel weight specific impulse of ethylene was greater than that of the slurry. However, the curves for the experimental data tend to converge as the fuel-air ratio was increased. This effect is attributed to two factors. The ideal impulse curves converge at the higher fuel-air ratios. Also, the air specific impulse efficiency decreased for ethylene and increased for the slurry with increasing fuel-air ratio. At an air specific impulse of 159 seconds, which was the maximum obtained with ethylene, the fuel weight specific impulses of the ethylene and the slurry were 2350 and 2000 seconds, respectively.

Fuel volume specific impulse, which is a measure of the fuel volume consumption, is presented on figure 13(b) as a function of the air specific impulse. A specific gravity of 18.3 pounds per cubic foot was used for the ethylene volume impulse computation. This specific gravity had been obtained when the fuel tank was pressurized to 1200 pounds per square inch. The fuel volume specific impulse of the slurry was 2.1 and 3.1 times greater than that of ethylene at air specific impulses of 120 and 159, respectively. At air specific impulse values of 150 to 170, the experimental fuel volume impulse of the slurry varied from 10 percent lower to approximately the ideal for octene-1.

The fuel volume specific impulse is a significant parameter when applied to vehicles that have a small ratio of fuel weight to gross vehicle weight. For example, the Langley vehicle has an ethylene fuel to gross weight ratio of 0.1. Hence, a large increase in volume specific fuel consumption can effect a correspondingly large increase in fuel load with only a small increase in vehicle gross weight.

The last portion of a gaseous fuel in a fuel-pressurized system is unavailable for combustion because of the supply system used. In contrast, the slurry fuels require a pumping facility. These penalties must be considered when the fuel volume and fuel weight specific impulses are related to a specific application. Although magnesium slurries have been successfully pumped with a positive-displacement pump, gas pressurization of the slurry for small-vehicle applications appears promising and has been investigated (see appendix C).

Gross thrust coefficients were computed from the data of figure 13(a) by the method shown in the Data Reduction section and are presented on figure 14 as a function of equivalence ratio. An experimental simulated thrust coefficient of 0.5 was obtained at an equivalence ratio of 0.4 for both the ethylene and the slurry fuels. At stoichiometric equivalence ratio, the coefficients for ethylene and the slurry were 1.03 and 1.33, respectively. The slurry coefficients were greater than the ideal coefficients for octene-1 for equivalence ratios greater than 0.58.

An ordinate scale of net thrust coefficient is presented on figure 14. The net thrust coefficient is equal to the gross thrust coefficient less one half the drag coefficient of the twin-engine Langley vehicle. This coefficient is a measure of the acceleration capability of a vehicle. Both slurry and ethylene fuels provide positive net thrust coefficients over a wide range of equivalence ratios. The maximum net thrust coefficient obtained with the slurry was 1.01 and was 1.43 times the maximum obtained with ethylene.

Comparison of combustor pressure data. - Figure 15 presents combustor-inlet stagnation pressure as a function of mass flow. The mass flows for the slurry data were computed from the faired curves in figure 8, and the ethylene data are from reference 6 for a comparable 6-inch-diameter choked-exit-nozzle throat. At a constant air flow and comparable gross thrust coefficients, the combustor-inlet pressure generally was lower for the slurry than for the ethylene fuel.

Comparison of fuel-ignition data. - The ethylene ignition system (ref. 5) used two small ignition squibs and a magnesium starting disk which blocked 69 percent of the combustor area. The disk lowered the starting combustor-inlet velocity and allowed proper mixing of the fuel and air prior to ignition. Approximately 0.7 second after ignition, the disk burned away and the combustor pressure was at normal operating conditions.

The slurry was ignited by one large flare without the aid of a starting disk. The flare was ignited and the fuel turned on. Table III lists slurry performance data and the time from the start of fuel flow. The first point listed after time zero represents the time interval required to bring the engine to operating conditions. The longest time required was 3.1 seconds for the five tests covering a range of starting equivalence ratios from 0.65 to 0.90. In each run, about 1.5 seconds had elapsed before the thrust trace began to rise. The major portion of this time was required to fill the fuel system downstream of the orifice restriction. The starting characteristics of the slurry system appeared to be satisfactory over the range of equivalence ratios examined.

#### SUMMARY OF RESULTS

1. The following results were obtained in the application of a 50 percent magnesium slurry to a flight-type, 6.5-inch-diameter ram-jet engine evaluated in a connected-pipe facility:

- a. A combustor was developed for slurry fuels that provided acceptable combustion performance for equivalence ratios between 0.39 and 0.95. Combustion limits were not determined.



b. An air specific impulse of 178 seconds was obtained at the 0.95 equivalence ratio.

c. Air specific impulse efficiencies of 87 and 96 percent were obtained at equivalence ratios of 0.40 and 0.95, respectively. Combustor efficiencies of 66 and 86 percent were computed at the same equivalence ratios.

d. Ignition and starting of the ram-jet engine were successfully accomplished by an electrically fired flare over a range of equivalence ratios of 0.65 to 0.90.

e. The durability of all combustor parts was satisfactory for a test duration of 78 seconds under severe durability test conditions.

f. The deposition of solid products of combustion in the combustion chamber and exit nozzle was confined to a thin layer.

2. The following results compare the performance of the slurry fuel to that of ethylene fuel, both evaluated under similar conditions. The ethylene data were obtained from free-jet and flight tests reported previously.

a. The thrust coefficient for slurry fuel exceeded that for ethylene at equivalence ratios greater than 0.4 for a simulated free-stream Mach number of 2.3 and for altitudes above the tropopause. At these free-stream conditions, the maximum net thrust coefficient obtained with the slurry was 1.01, 43 percent more than the maximum obtained with ethylene.

b. At constant air flow and comparable thrust coefficients, the combustor-inlet pressure was generally lower for the slurry than for the ethylene fuel.

c. The fuel volume specific impulse of the slurry was 2.1 and 3.1 times greater than that of ethylene at air-specific impulse values of 120 and 159 seconds, respectively.

d. The fuel weight specific impulses of ethylene and slurry fuels were 2350 and 2000 seconds, respectively, and for the maximum air specific impulse obtained with the ethylene, 159 seconds.

#### CONCLUDING REMARKS

The combustor developed for use with slurry fuels provided acceptable combustion performance over the full range of combustor-inlet conditions

investigated. These conditions simulated most of the range of combustor-inlet conditions that probably would be encountered during flight tests of the vehicle. Furthermore, combustion performance comparisons made for slurry and ethylene fuels in similar engines indicated that slurry fuel could provide appreciable increases in maximum velocity, acceleration, and range of the vehicle.

Lewis Flight Propulsion Laboratory  
National Advisory Committee for Aeronautics  
Cleveland, Ohio, March 30, 1953

2755

CI-3

## APPENDIX A

EFFECT OF ENGINE CONFIGURATION AND FUEL VARIABLES ON  
COMBUSTION PERFORMANCE

Development procedures. - The program presented herein was directed towards the development of a slurry-fueled combustor for the flight vehicle. This objective probably could have been attained with the least difficulty by using the highly reactive, grade C powder throughout the investigation. Unfortunately, this powder was available in only a limited quantity and had to be reserved for the latter phases of the program. The coarse powder showed sufficient variations in average particle size to require two separate designations (grades A and B).

The diffuser was designed to be used in flight with a 6-inch-diameter exit nozzle; however, a 5.66-inch nozzle was used in the initial phase of the present investigation to provide low combustor velocities and stable combustion for a variety of engine configurations.

Exploratory tests indicated that variations in fuel-injection and flame-stabilizing apparatus had large effects on combustion performance. Occasionally, simultaneous modifications were made to several engine components. The results presented herein are restricted to the configurations that either performed satisfactorily or were so related to other configurations that a coherent analysis of the data could be made. The flame-holder and fuel-injection configurations considered herein are illustrated in figures 16 and 17, respectively. The eight fuel injector configurations are divided into two general schemes. The variable-port-area injector (fig. 4) was used with injector types A through E (fig. 17(a)). Four of these injectors utilized fuel-impingement surfaces mounted in the air stream. The second fuel injector scheme employed small, round orifices in conjunction with high injector pressures (approximately 600 lb/sq in.). The flow-restriction orifice was not used in these tests since the injection orifices acted as the flow restrictors. The locations of the high-pressure orifices are shown in figure 17(b).

Tests conducted using a 5.66-inch-diameter nozzle. - Performance data for four flame holders of types A, B, and C of figure 16 are presented in figure 18. A type C fuel injector (fig. 17) was used for this series of tests. Flame holders with funnels were designed to concentrate the atomized fuel in the recirculatory zone of the flame holder. The funnel flame holder and the gutter flame holder each had a projected area blockage of 40 percent; however, the friction loss of the funnel was smaller than that of the gutters. Although the data scatter was large, the performance level for these two flame holders

was approximately the same. Two type-C flame holders were tested. The performance of the one with 40 percent area blockage was lower than that of types A and B. This effect was attributed to the reduced width of the funnels and gutters, which reduced their effectiveness. The best performance was obtained with a type C, 46-percent-area-blockage flame holder having funnels and gutters that were 25 percent wider than those of the previous flame holder. Nearly theoretical performance was achieved at equivalence ratios greater than 0.8, but the efficiency decreased rapidly at leaner mixtures until blow-out was reached at 0.48 equivalence ratio.

The series of tests described was conducted during a period in which the fineness of the magnesium powder was varied. Combustion performance was not appreciably affected when grade A magnesium, the coarser of the two powders, was substituted for grade B magnesium.

Although several flame holders other than types A, B, and C were investigated, only one is of sufficient interest to mention. The slotted-can flame holder, D (fig. 16), is similar to a type used in gasoline-fueled ram-jet engines. This flame holder would support combustion over a limited range of equivalence ratios; however, the inner surfaces were so effectively bathed in the flame that the conical portion rapidly melted away.

Effort was next directed towards improving the lean-mixture performance by modifying the fuel-stratification technique. Thrust performance data for fuel injector configurations A, B, and C of figure 17 are presented on figure 19. The type-A flame holder (fig. 16) was used for this series of tests. Successive improvements in impulse level and blow-out limits were obtained when the injector configuration was varied from type A through type C. Results of a series of tests, using three types of high-pressure fuel jet (fig. 17) and a type-C flame holder with 46 percent blocked area, are presented on figure 20. Fuel-injection pressure ranged from 200 to 600 pounds per square inch. Type-F injection resulted in unstable combustion and type-H injection resulted in stable combustion at a very low impulse level. For the high-pressure injector tests, the best performance was obtained with the type-G configuration. A comparison of figures 18 and 20 shows that the type-G injector exhibited lower air specific impulse than the type-C injector when both types were tested with the same flame holder.

After tests with fuel injector types A, F, and H, fuel traces were found on the diffuser and combustor walls. With injector types B, C, and G, fuel traces were found on the diffuser inner body, which indicated that the fuel assumed a path much closer to the axis of the engine. In the latter case more fuel entered the portals of the flame holder, which caused a locally rich zone behind the flame holder and resulted in improved performance. The performance of the type-C injector was better than that of either types B or G probably because of improved atomization of the fuel spray by the air stream.

Data for a 3-inch-long sleeve, type-D injector of figure 17 are presented in figure 21. For comparison, a curve of the data obtained with the type-C injector is shown on the same figure. Impulse performance reproducibility for the two runs made with the sleeve configuration was very good. In addition, lean operation was extended to an equivalence ratio of 0.4 and, when compared with the type-C injector, the sleeve configuration provided improved impulse performance at equivalence ratios less than 0.75.

Oxide deposits on runs 79 and 80 (fig. 21) were the largest observed during the course of the investigation. A photograph (fig. 22), taken after run 79, shows the deposits adhering to the flame holder and nozzle. The duration of each run was 4 minutes, or approximately twice the burning time for previous tests in which stable burning was achieved. The oxide deposition on the nozzle developed in a progressive fashion and the combustor-inlet velocity at a given equivalence ratio decreased accordingly. For example, at an equivalence ratio of 0.7 and with a choked exit nozzle, the first air-flow traverse resulted in a velocity of 200 feet per second, whereas on the sixth (final) traverse, the velocity was only 170 feet per second.

Stable and reproducible impulse performance, achieved over a fairly wide range of equivalence ratios, climaxed the first phase of the program. Performance at the leanest equivalence ratio of interest was still unsatisfactory, and solid deposition was excessive.

Tests conducted with 6-inch-diameter nozzle. - The remaining runs presented in this report were conducted with a 6-inch-diameter nozzle and a type-C flame holder with 46 percent blocked area.

Two series of tests (fig. 23), in which the atomization sleeve length was 3 and 4.5 inches, respectively, were conducted using grade C magnesium powder in the slurry.

The series of runs with the 3-inch sleeve (fig. 23(a)) resulted in air specific impulse efficiencies ranging from 99 to 87 percent at an equivalence ratio of 0.7. On the first run, higher combustor pressures and wall temperatures than had been previously recorded tended to substantiate the high impulse values obtained. Unfortunately, the performance was lower for the two subsequent runs of this series. Observation of the combustor after each run indicated that oxide formation was negligible and could not account for the lack of reproducibility in these tests. Undetected differences in the three fuel batches used in these tests may be responsible for the resulting three separate impulse levels.

Impulse data for five runs using a 4.5-inch atomization sleeve are presented in figure 23(b). The results of these tests are presented in

greater detail in the body of the report. Stable combustion was maintained at equivalence ratios leaner than heretofore possible. Reproducibility of performance was considerably improved by use of the longer sleeve; however, none of the runs resulted in so high an impulse level as was recorded for the best run shown on figure 23(a).

Data are presented in figure 24 for two runs in which the slurry contained grade B magnesium. A 4.5-inch sleeve injector, considered to be the best type evolved during the development program, was used. The impulse level of run 91 was slightly higher than that of run 93 possibly because of higher inlet-air temperature. The blow-out velocity on each run was 300 feet per second. Figure 24 also contains a curve for the data (fig. 23(b)) obtained with grade C powder. This powder markedly improved the impulse level and extended the lean operational limits.

General comparisons. - Separately, the variations in flame holders, injection methods, and exhaust nozzles had a pronounced effect on combustor performance.

Of the flame holders tested, the 46-percent-blocked-area, funnel-gutter configuration provided the best source of flame stabilization.

The results of the injector-configuration variations indicated that the 4.5-inch sleeve permitted stable operation at leaner mixture strength than any of the other types tested. Although the forward-splash, type-C injector provided nearly theoretical impulse performance at equivalence ratios greater than 0.8, these tests were conducted with the smaller exhaust nozzle and hence cannot be directly compared to the 4.5-inch-sleeve data.

A tabulation of the data of figures 21 and 24 serves to illustrate the effect of exit-nozzle diameter on combustion performance:

Exit-nozzle diameter, in.	Fuel injector		Air specific impulse at 0.8 equivalence ratio	Lean blow-out equivalence ratio
	Type	Sleeve length, in.		
5.66	D	3.0	166	0.39
6.00	E	4.5	160	.55

The slurries used in these tests contained grade B powder. The type-E injector was shown previously to exhibit better combustion characteristics at lean mixtures than the type-D injector. From the table it can be seen that the larger nozzle used in combination with the type-E injector decreased the impulse level and increased the tendency of flame blow-out. Consequently, the enlarging of the exit nozzle seriously

reduced the combustion performance. In general, the greatest oxide deposits were associated with use of the smaller nozzle and the coarser powder. Oxide coatings on the 6-inch nozzle were confined to a spalling layer that was in the order of 1/16 inch thick.

Whereas the engine configuration was deliberately modified throughout the course of the investigation, the fuel and operating procedure were not always so subject to control. A discussion of these variables follows.

An over-all inspection of the test data does not show any correlation between combustion performance and fuel viscosity. This effect is not surprising since the viscosities of these fuels decrease with shear rate (ref. 8). Therefore, the high viscosity values (table II), as measured by a viscometer employing low shear rates, are not necessarily indicative of the actual fluidity of the slurries at the injector station.

Small-scale combustor studies (ref. 11) show that grade B powder is less reactive, combustionwise, than the finer grade C powder. Similar effects were observed in the present investigation, when the powder was changed from grade B to grade C (fig. 24). No measurable difference in performance was noted when the metal component of the slurry was changed, for a brief period, from grade B to the somewhat coarser grade A magnesium powder.

On figures 18, 19, and 24, the inlet-air temperature is shown to deviate considerably from run to run. Although a systematic study of the effect of inlet-air temperature was not undertaken, the data indicate that combustion performance was improved by moderate increases in inlet-air temperature. This effect was further substantiated by several tests, made from time to time, in which stable combustion was not achieved at an inlet-air temperature of 60° F.

## APPENDIX B

## PRECISION OF DATA AND RELIABILITY OF RESULTS

Measurement of stream momentum. - The primary parameter used to express combustor performance was air specific impulse. In order to determine air specific impulse it was necessary to determine the total momentum of the exhaust gases at the nozzle throat. This was accomplished by use of a thrust barrel, shown in figure 25. The short cylindrical duct was not a part of the installation but was included on the figure for convenience in presenting the momentum analyses of the system.

The pressure at station 12 is considered to be the ambient pressure exerted on all vertical surfaces of the thrust barrel exclusive of section X-X (fig. 25). The reaction, B, measured by the thrust barrel is

$$m_{11}V_{11} + p_{11}A_{11} - p_{12}A_{11} \quad \text{where } m = W/g$$

From the principle of conservation of momentum

$$m_{11}V_{11} + p_{11}A_{11} = (p_gA_g + m_gV_g) + (p_{10}A_{10} + m_{10}V_{10})$$

Therefore, the reaction measured by B is equal to

$$(p_gA_g + m_gV_g) + (p_{10}A_{10} + m_{10}V_{10}) - p_{12}(A_g + A_{10})$$

Since the term  $(p_gA_g + m_gV_g)$  is the stream momentum of the combustion products at the nozzle exit, the thrust equation becomes

$$F_g = B - (p_{10}A_{10} + m_{10}V_{10}) + p_{12}(A_g + A_{10})$$

The ambient pressure  $p_{12}$  is essentially a total pressure since the area of any flow channel bounded by the barrel and the outer shell is very large. The induced flow  $m_{10}$  results from the pressure difference between  $p_{12}$  and  $p_{10}$ . For small pressure differences, the induced gas flow can be expressed by the incompressible Bernoulli equation

$$p_{12} - p_{10} = \frac{\rho_{10}V_{10}^2}{2g} = \frac{m_{10}V_{10}}{2A_{10}}$$



which is more conveniently stated as

$$\dot{m}_{10}V_{10} = 2(\Delta p)A_{10}$$

Substitution of these relations into the aforementioned thrust equation yields

$$F_9 = B - p_{12}A_{10} + (\Delta p)A_{10} - 2(\Delta p)A_{10} + p_{12}A_9 + p_{12}A_{10} =$$

$$B + p_{12}A_9 - (\Delta p)A_{10}$$

Areas  $A_9$  and  $A_{10}$  are approximately equal, but the pressure difference  $\Delta p$  is much smaller than  $p_{12}$ . If it is assumed that  $\Delta p$  is negligible, the thrust equation becomes

$$F_9 = B + p_{12}A_9$$

A series of tests was conducted to determine the validity of this equation. Metered quantities of air at 2 to 5 atmospheres pressure were discharged through a long cylindrical pipe attached to a convergent nozzle mounted in the position normally occupied by the engine combustor and nozzle. The pipe and nozzle diameter were smaller than those of the engine in order to obtain the desired pressure with a limited air supply. The stream momentum computed from the air flow rate and stagnation pressure, assuming idealized one-dimensional flow relations, was compared to the stream momentum expressed as  $B + p_{12}A_9$ . The two methods of momentum determination showed an agreement that was within the accuracy of the instrumentation.

Accuracy of instrumentation. - The limited availability of magnesium powder, particularly the grade C material, necessitated obtaining the maximum of data for a given set of operating conditions. Nonthermal equilibrium operation and the use of fast-response instrumentation was necessary.

Calibration data indicate the over-all accuracy of the oscillograph system to be 2 percent of the values measured. The remainder of the instrumentation had an even higher degree of accuracy.

In addition to complying with the calibration procedure outlined previously, the instrumentation was thoroughly recalibrated immediately prior to run 97. The data for run 97 are shown on figures 5 through 8 to be in close agreement with the data obtained for the other runs of this series.

Precision of fuel-flow rate determination. - The method of fuel-flow rate determination, calculated from the slope of the fuel-tank weight against time flow, resulted in probable errors of approximately 3 percent. These errors were larger than the errors caused by instrument inaccuracy since only part of the full instrument range was used in measuring one constant flow rate.

2755  
4-10  
Effect of transient pressure conditions. - Since the inlet plenum is in effect a storage tank, the combustor-inlet flow rate for unsteady-state conditions differs from the orifice-measured flow rate. Another air-flow error could be caused by combustor pressure fluctuations traveling upstream into the plenum. Furthermore, these pressure fluctuations might have a detrimental effect on combustion performance. A simple method of determining the possible existence of these effects can be shown by means of figure 26. The diffuser total pressure ratio  $P_7/P_0$  and the ratio of the air flow required to choke the diffuser to the measured (orifice) air flow are plotted as a function of combustor-inlet Mach number  $M_c$  for the data of table III. The air-flow ratio should be unity at inlet velocities greater than that for choked flow. At Mach numbers greater than 0.19, the diffuser was choked and the maximum deviation of the air flow ratio data from unity was 4 percent. Therefore, the air flow rate at the orifice was taken as the air flow rate at the combustor inlet for the chosen data points. The transition from choked to unchoked diffuser flow occurred at an equivalence ratio of approximately 0.65. Impulse performance (fig. 5) did not appear to be affected by this phenomenon.

~~CONFIDENTIAL~~

## APPENDIX C

## FUEL-FLOW BENCH TESTS FOR FLIGHT APPLICATION

A simple fuel system has been proposed for use in short-range flight vehicles similar to the vehicle described in references 5 and 6. The principle of the system operation is as follows: The tank is partly filled with fuel and the remaining volume is charged with an inert gas. The orifice flow restriction is chosen to provide the desired initial fuel flow rate at the initial tank pressure. As fuel flows from the tank, the pressure decreases and thereby reduces the flow rate. Some control over the slope of the fuel flow decay curve is possible by suitable choice of the initial fuel to inert-gas volume ratio for a given tank volume. This method of flow control is believed to be sufficiently flexible to provide the flow rates required for some flight paths of interest.

A bench-test investigation was undertaken to check the operation of the proposed system for a twin-engine application and to check the flow properties of the slurry fuels. The apparatus is illustrated on figures 27 and 28. The fuel tank and starting valve body are identical to those used in the vehicle reported in reference 5; however, the starting valve was operated pneumatically rather than by the firing of squibs in order to permit both opening and closing of the valve. A spring-loaded cylinder valve of the type shown in figure 4 was mounted in each of the 5.5-inch-diameter reservoirs. Fuel, discharged through these valves, produced an upward movement of the pistons and the markers rigidly connected to the pistons. The length of fuel line between the fuel tank and injection valves was approximately the same as that for the fuel system reported in references 5 and 6.

For each test, a measured amount of slurry containing equal parts by weight of magnesium and MIL-F-5624A, grade JP-3 fuel plus additive was placed in the 1.37-cubic-foot tank. Additional fuel was placed in each reservoir to a depth sufficient to cover the cylinder valves. The pistons were forced down until all the air and some fuel flowed up the marker pipes. The pipes then were capped to seal the system. The tank was pressurized to 1000 pounds per square inch and the nitrogen supply was then closed.

Photographs of the pressures, time, and marker positions were obtained throughout each test at intervals of approximately 1.3 seconds. Marker position was converted to volume and then to fuel weight. The fuel flow rates were computed from the slopes of the fuel weight-time curves.

Three tests were conducted with a 0.105-inch-diameter restricted-approach orifice mounted in each outlet of a 1/2-inch T-fitting dividing the flow to the two cylinder-valve assemblies. Flow rate and pressure data are presented in figure 29(a). Within the limits of experimental error, the flow was divided evenly between the two reservoirs. The two grade B magnesium powder slurries tested differed widely in viscosity but exhibited similar flow rates. The grade C powder slurry gave flow rates approximately 7 percent greater than the grade B powder slurries. The discontinuity in several of the injector pressure curves was probably caused by friction of the pistons in the cylinder valves.

Three tests were conducted using one reservoir and a 0.125-inch-diameter orifice (fig. 27) which did not have a restricted approach section. These data are presented in figure 29(b). The flow rate, with the orifice mounted in a 1/2-inch straight fitting threaded into the fuel tank, was somewhat greater than when the orifice was mounted in one end of the T-fitting. In contrast to the data of figure 29(a), the flow rates were not affected by a decrease in powder particle size. Viscosity differences caused no differences in flow rates.

The area discharge coefficients for the bench test data are presented on figure 30 as a function of orifice pressure drop. The 0.125-inch-diameter orifice resulted in considerably lower discharge coefficients than the smaller orifice with the restricted approach; however, as noted previously, the larger orifice appeared less sensitive to the metal particle size. When the orifice was mounted in a straight fitting, the discharge coefficient was much more nearly independent of pressure than when the orifice was mounted in the end of a T-fitting.

The fuel system appears to be suitable for use with slurry-type fuels for initial flight investigations.

#### REFERENCES

1. Lord, Albert M.: An Experimental Investigation of the Combustion Properties of a Hydrocarbon Fuel and Several Magnesium and Boron Slurries. NACA RM E52B01, 1952.
2. Tower, Leonard K., and Branstetter, J. Robert: Combustion Performance Evaluation of Magnesium-Hydrocarbon Slurry Blends in a Simulated Tail-Pipe Burner. NACA RM E51C26, 1951.
3. Hill, Paul R., and Gammal, A. A.: An Analysis of Ducted-Airfoil Ram Jets for Supersonic Aircraft. NACA RM L7124, 1948.

4. Faget, Maxime A., Watson, Raymond S., and Bartlett, Walter A., Jr.: Free-Jet Tests of a 6.5-Inch-Diameter Ram-Jet Engine at Mach Numbers of 1.81 and 2.00. NACA RM L50L06, 1950.
5. Faget, Maxime A., and Dettwyler, H. Rudolph: Initial Flight Investigation of a Twin-Engine Supersonic Ram Jet. NACA RM L50H10, 1950.
6. Dettwyler, H. Rudolph, and Bond, Aleck C.: Flight Performance of a Twin-Engine Supersonic Ram Jet From 2,300 to 67,200 Feet Altitude. NACA RM L50L27, 1951.
7. Breitwieser, Roland, Gordon, Sanford, and Gammon, Benson: Summary Report on Analytical Evaluation of Air and Fuel Specific-Impulse Characteristics of Several Nonhydrocarbon Jet-Engine Fuels. NACA RM E52L08, 1953.
8. Gibbs, James B., and Cook, Preston N., Jr.: Preparation and Physical Properties of Metal Slurry Fuels. NACA RM E52A23, 1952.
9. Rudnick, Philip: Momentum Relations in Propulsive Ducts. Jour. Aero. Sci., vol. 14, no. 9, Sept. 1947, pp. 540-544.
10. Simon, Dorothy M., and Wong, Edgar L.: The Velocities over a Wide Composition Range for Pentane-Air, Ethylene-Air, and Propyne-Air Flames. NACA RM E51H09, 1951.
11. Lord, Albert M., and Evans, Vernida E.: Effect of Particle Size and Stabilizing Additives on the Combustion Properties of Magnesium Slurry. NACA RM E52K12, 1953.

TABLE I. - SPECIFICATIONS AND ANALYSIS OF  
HYDROCARBON CARRIER FUEL

	Specifications MIL-F-5624A (JP-3)	Analysis of carrier fuel
A.S.T.M. distillation D 86-46, °F		
Initial boiling point		106
Percent evaporated		
5		144
10		177
20		218
30		246
40		272
50		299
60		323
70		349
80		379
90	400 (min.)	417
95		445
Final boiling point	600 (max.)	479
Residue, percent	1.5 (max.)	0.9
Loss, percent	1.5 (max.)	0.6
Aromatics, percent by volume		
A.S.T.M. D-875-46T	25 (max.)	8.5
Specific gravity	0.728 (min.)	0.755
Reid' vapor pressure, lb/sq in.	5 - 7	6.2
Hydrogen-carbon ratio		0.171
Net heat of combustion, Btu/lb	18,400 (min.)	18,725



TABLE II. - DESCRIPTION OF FUELS

[All slurries are 50 percent magnesium by weight in MIL-F-5624A grade JP-3 fuel]

Batch	Powder grade	Viscosity <sup>a</sup> , centipoise	Stability time <sup>b</sup>	Used in run
	B			8,9,10,13,14
	B			19,20,21
4	A		Unstable	22
11	A		Unstable	29
14	A		Unstable	30
15	A		Unstable	31
48	B		Unstable	70
49	B		Unstable	71
50	B		Unstable	72
52	B	560	Unstable	73
53	B	840	Unstable	74
54	B	5,060	6 Months	75
57	B	1,900	1 Day	79
58	B	3,000	4 Days	80
61	C	17,000	5 Days	81
65	C	5,600	1 Month	84
68	C	650	7 Days	86,87,88
69	C	1,500	1 Day	89,90
71	B	15,600	2 Months	91
74	B	3,800	2 Days	93
81	C	740	3 Hours	97

<sup>a</sup>Viscosity was obtained with a Brookfield viscometer.

<sup>b</sup>Time in storage before a thin layer of clear liquid forms at the top of fuel.



2755

TABLE III. - SUMMARY OF BEST COMBUSTION DATA FOR 6.6-INCH RAM JET

[Slurry: 50 Percent Magnesium grade C powder in MIL-W-5624A grade JP-3 fuel. Configuration: 6-inch-diameter nozzle; flame holder C, 46 percent blocked area; fuel injector, variable-area slots, type E]

Run	Time from start of fuel flow, sec	Fuel tank nitrogen pressure, lb/sq in. abs	Fuel flow, lb/sec	Combustion air flow, lb/sec	Equivalence ratio	Inlet plenum pressure, lb/sq in. abs	Static pressure at station 7, lb/sq in. abs	Static pressure at station 8, lb/sq in. abs	Exit plenum pressure, lb/sq in. abs	Inlet stagnation temperature, °F	Barrel thrust, lb	Air specific impulse, sec	Combustor wall temperature $\frac{1}{2}$ in. upstream of combustor exit, °F
87	0	600	0	8.00	0	44.1	20.4	17.1	15.2	325	---	---	315
	3.0	↓	↓	7.82	.768	47.1	41.7	31.7	18.8	327	855	168	380
	5.8	↓	↓	8.74	.693	50.3	44.2	33.5	18.5	332	948	162	480
	8.8	↓	↓	9.41	.648	53.3	48.3	35.2	18.5	334	1018	158	590
	12.6	↓	↓	10.60	.573	58.2	49.4	37.6	18.5	338	1110	149	710
	16.3	↓	↓	12.22	.498	65.5	52.2	39.9	17.0	342	1192	137	840
	19.2	↓	↓	12.82	.473	70.4	53.5	41.1	17.2	344	1242	135	940
	23.0	↓	↓	12.52	.484	69.0	54.6	41.6	17.2	348	1263	140	970
	29.3	550	.852	12.20	.474	67.2	51.8	39.4	16.9	348	1157	134	940
	31.5	500	.611	12.08	.449	66.9	49.7	38.1	16.8	348	1102	131	830
	33.8	450	.379	11.96	.430	66.4	47.8	36.5	16.7	349	1052	128	820
	37.6	400	.536	11.83	.403	65.6	45.9	34.8	16.5	350	988	125	820
	40.0	375	.517	11.76	.390	65.2	44.7	32.9	16.4	350	952	120	820
	45.0	↓	↓	11.60	.395	64.5	42.1	32.2	16.4	350	917	119	820
	47.0	↓	↓	8.98	.480	58.3	39.4	30.5	16.2	350	835	130	850
	50.0	↓	↓	8.59	.533	50.0	37.0	29.2	16.0	350	738	139	1000
	55.0	↓	↓	7.89	.604	43.0	35.1	27.7	15.8	350	680	148	1100
88	0	800	0	13.8	0	72.1	23.2	21.4	18.2	264	---	---	255
	2.6	↓	↓	13.5	.649	71.6	62.6	46.6	17.6	266	1512	149	400
	7.1	↓	↓	13.0	.675	71.3	63.1	47.2	17.5	278	1535	156	630
	15.0	↓	↓	12.6	.695	69.6	62.0	46.4	18.1	286	1450	166	880
	17.8	↓	↓	12.8	.685	71.3	63.5	47.8	18.0	292	1500	167	940
89	0	600	0	8.23	0	45.7	18.6	16.8	14.9	322	---	---	310
	3.1	↓	↓	8.30	.897	50.6	45.0	34.5	18.3	325	978	174	380
	6.0	↓	↓	9.28	.804	55.2	48.5	37.1	18.6	324	1084	168	510
	10.0	↓	↓	11.20	.664	62.2	53.4	41.2	17.1	327	1255	165	690
	15.0	↓	↓	12.50	.596	68.9	57.1	44.7	17.6	330	1382	160	890
90	0	600	0	13.73	0	73.7	24.0	22.1	16.9	334	---	---	310
	1.5	↓	↓	13.60	.737	73.4	54.8	49.1	No thrust data for this part of test				920
	31.0	250	.583	12.20	.425	68.8	43.9	34.3	16.5	353	1025	122	920
	37.0	↓	↓	12.10	.428	67.9	42.6	33.7	16.5	353	970	119	880
	40.0	↓	↓	9.44	.548	54.7	39.7	30.9	16.1	352	848	138	900
	42.5	↓	↓	8.50	.608	49.3	36.6	29.5	16.0	352	800	148	980
	45.3	↓	↓	7.91	.654	45.7	37.0	28.5	15.8	351	747	151	1020
	48.1	↓	↓	7.01	.738	41.4	34.6	26.5	15.7	348	672	159	1090
	52.0	↓	↓	6.53	.817	39.1	32.7	25.1	15.5	347	610	166	1130
97	0	600	0	12.71	0	69.1	25.1	20.3	16.3	325	---	---	320
	2	↓	↓	12.40	.802	70.4	59.1	45.9	18.8	328	1503	164	430
	10	↓	↓	11.78	.836	69.1	60.8	45.9	18.0	337	1508	171	680
	20	↓	↓	11.37	.867	67.6	59.9	45.2	18.1	348	1447	172	1130
	30	↓	↓	11.14	.884	66.7	59.1	43.9	18.1	358	1400	172	1200
	40	↓	↓	10.90	.903	66.5	58.9	43.6	18.3	365	1372	173	1250
	50	↓	↓	10.71	.920	68.3	58.9	43.4	18.5	371	1364	178	1390
	60	↓	↓	10.65	.925	65.5	58.5	42.7	18.6	375	1358	177	1480
	70	↓	↓	10.55	.934	68.3	58.4	42.7	18.5	377	1346	177	1490
	78	↓	↓	10.40	.847	65.7	56.9	42.8	18.5	378	1355	181	1430

NACA



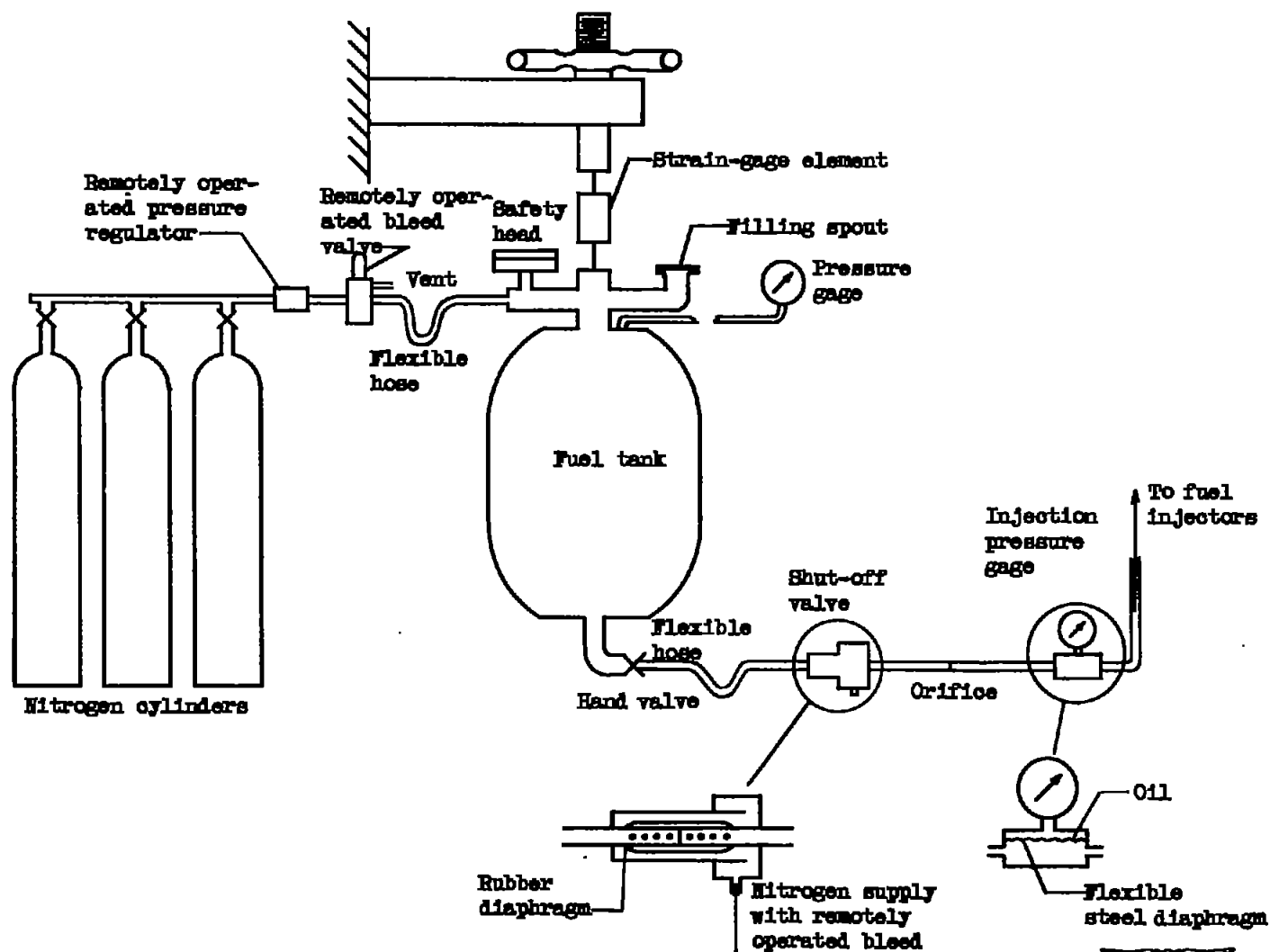


Figure 1. - Diagram of basic fuel system.

NACA  
CD-2979

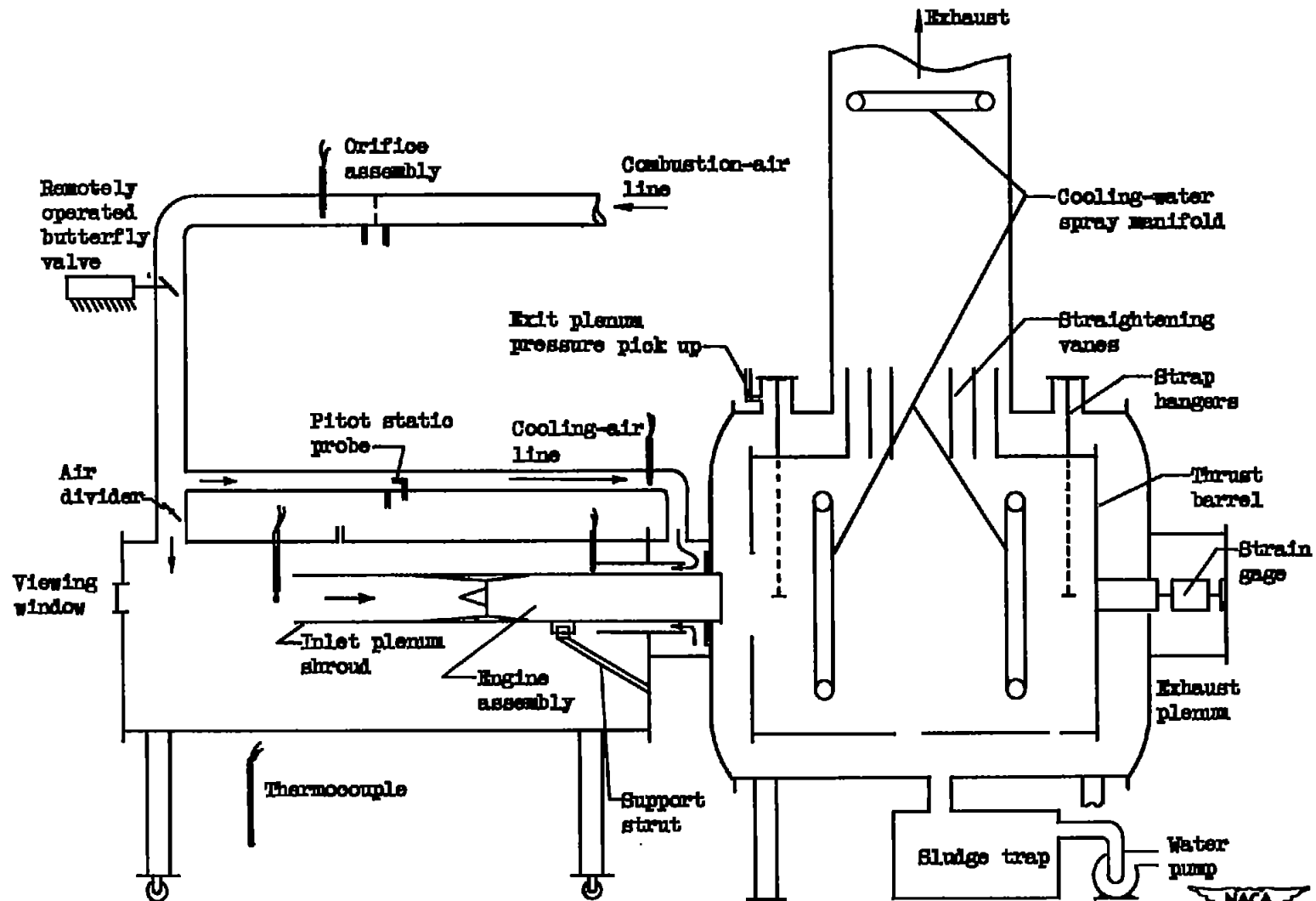


Figure 2. - Diagram of ram-jet installation.

NACA  
OD-2978

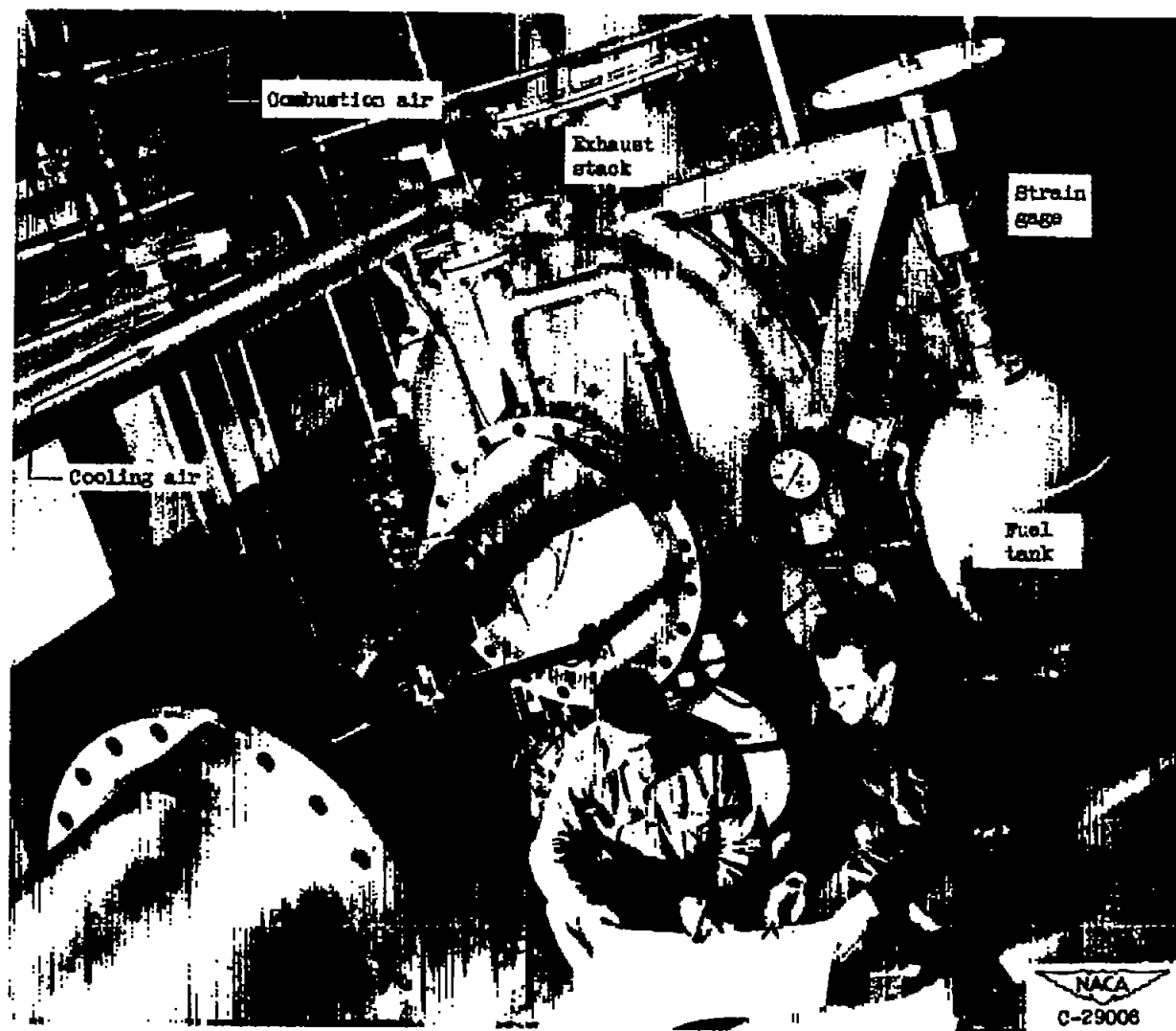


Figure 3. - Ram-jet installation. Inlet plenum retracted; inlet shroud removed.

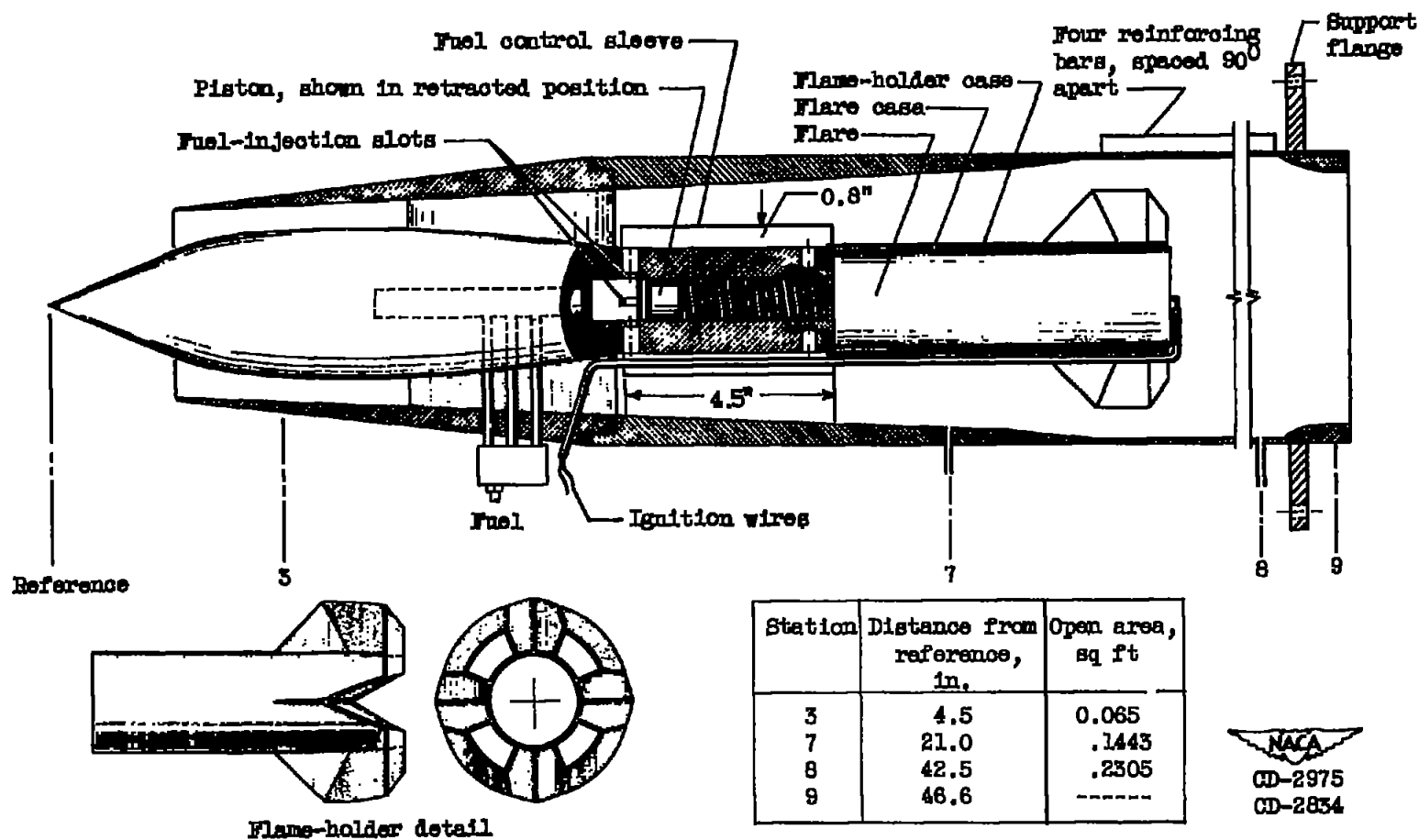


Figure 4. - Ram-jet engine.

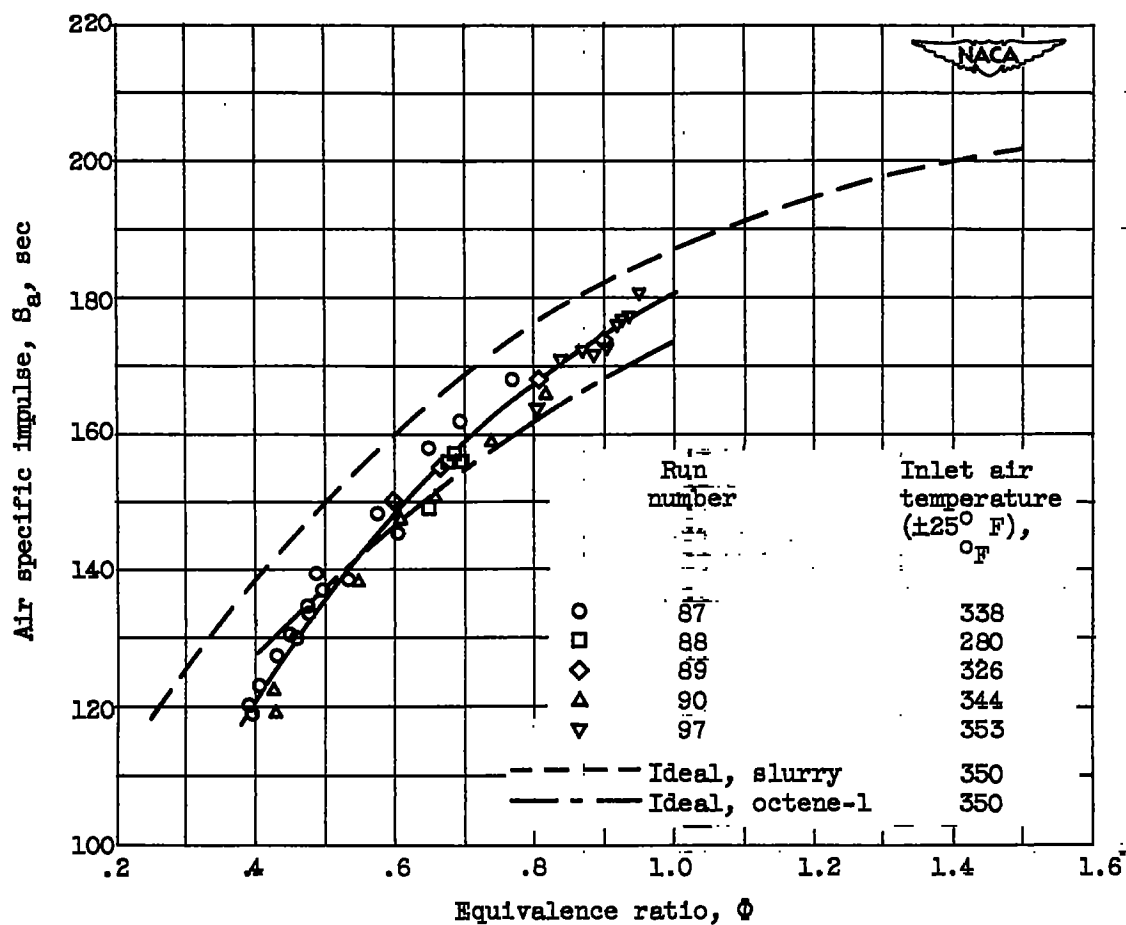


Figure 5. - Effect of equivalence ratio on air specific impulse for slurries containing 50 percent grade C magnesium in MIL-F-5624A grade JP-3 fuel. Flame holder C, 46 percent blocked area; fuel injector E; nozzle diameter, 6 inches.

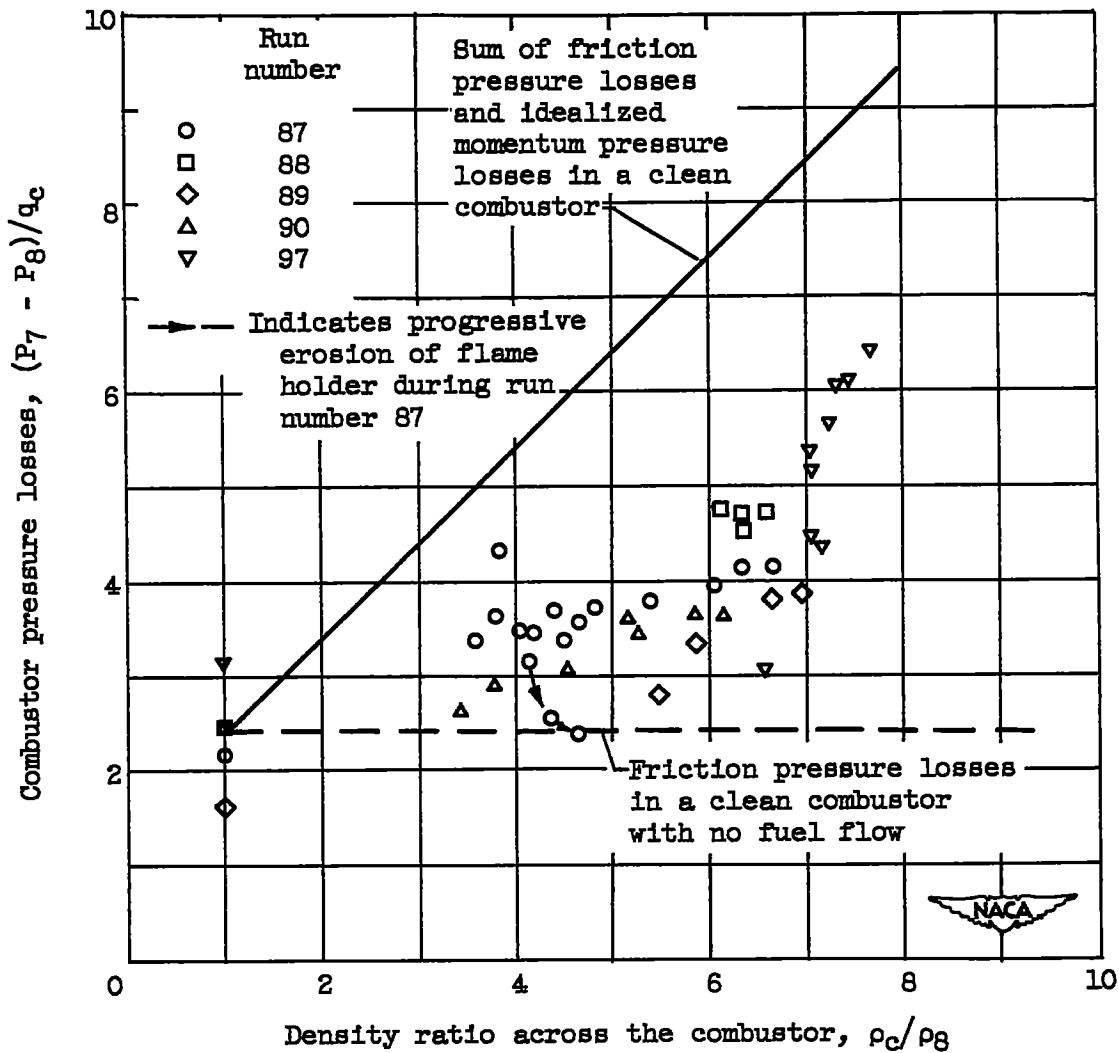


Figure 6. - Combustor pressure losses attributed to friction, momentum, and solid deposition for slurries containing 50 percent grade C magnesium in MIL-F-5624A grade JP-3 fuel. Flame holder C, 46 percent blocked area; fuel injector E; nozzle diameter, 6 inches.

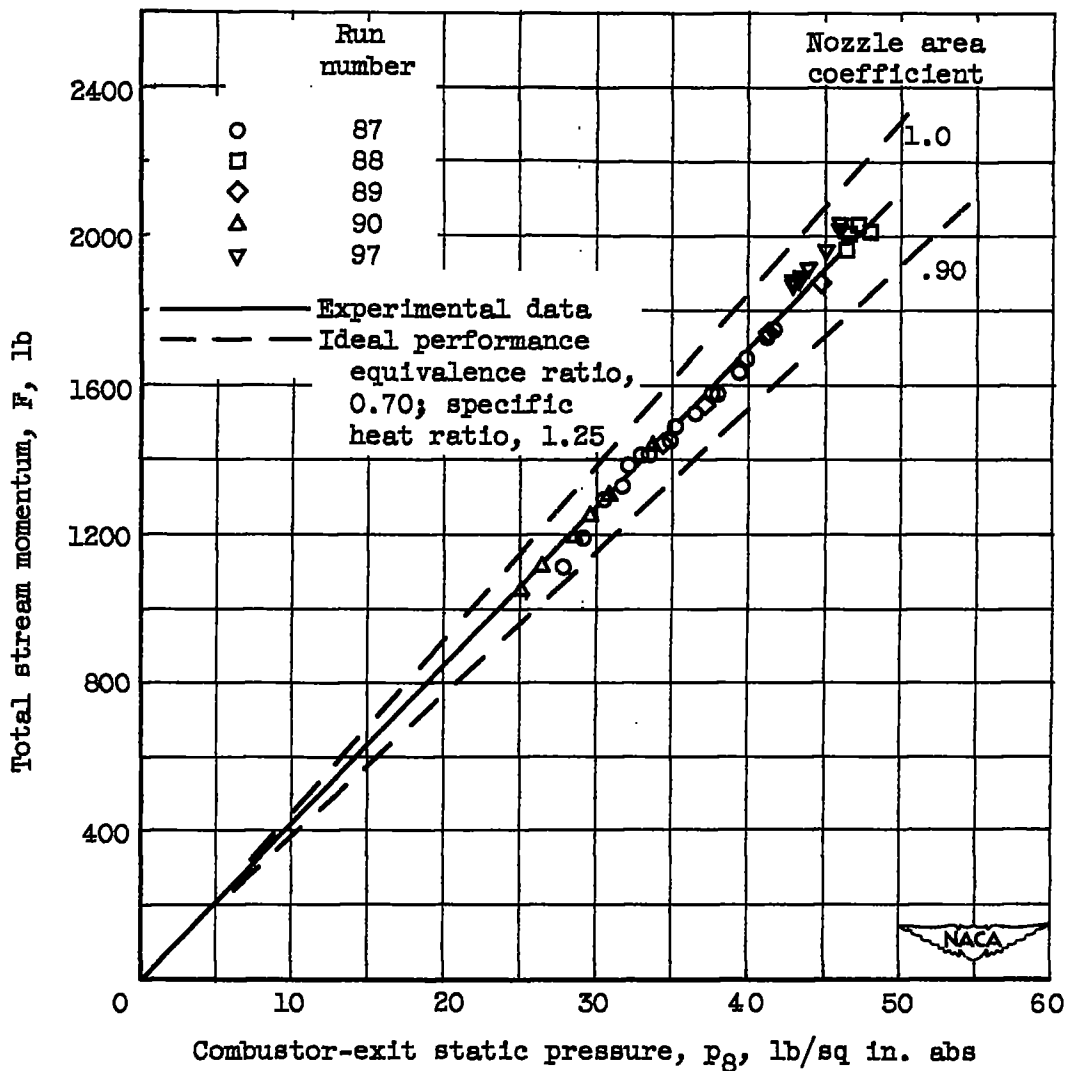


Figure 7. - Effect of combustor-exit pressure on total stream momentum at the nozzle exit for slurries containing 50 percent grade C magnesium in MIL-F-5624A grade JP-3 fuel. Flame holder C, 46 percent blocked area; fuel injector E; nozzle diameter, 6 inches.

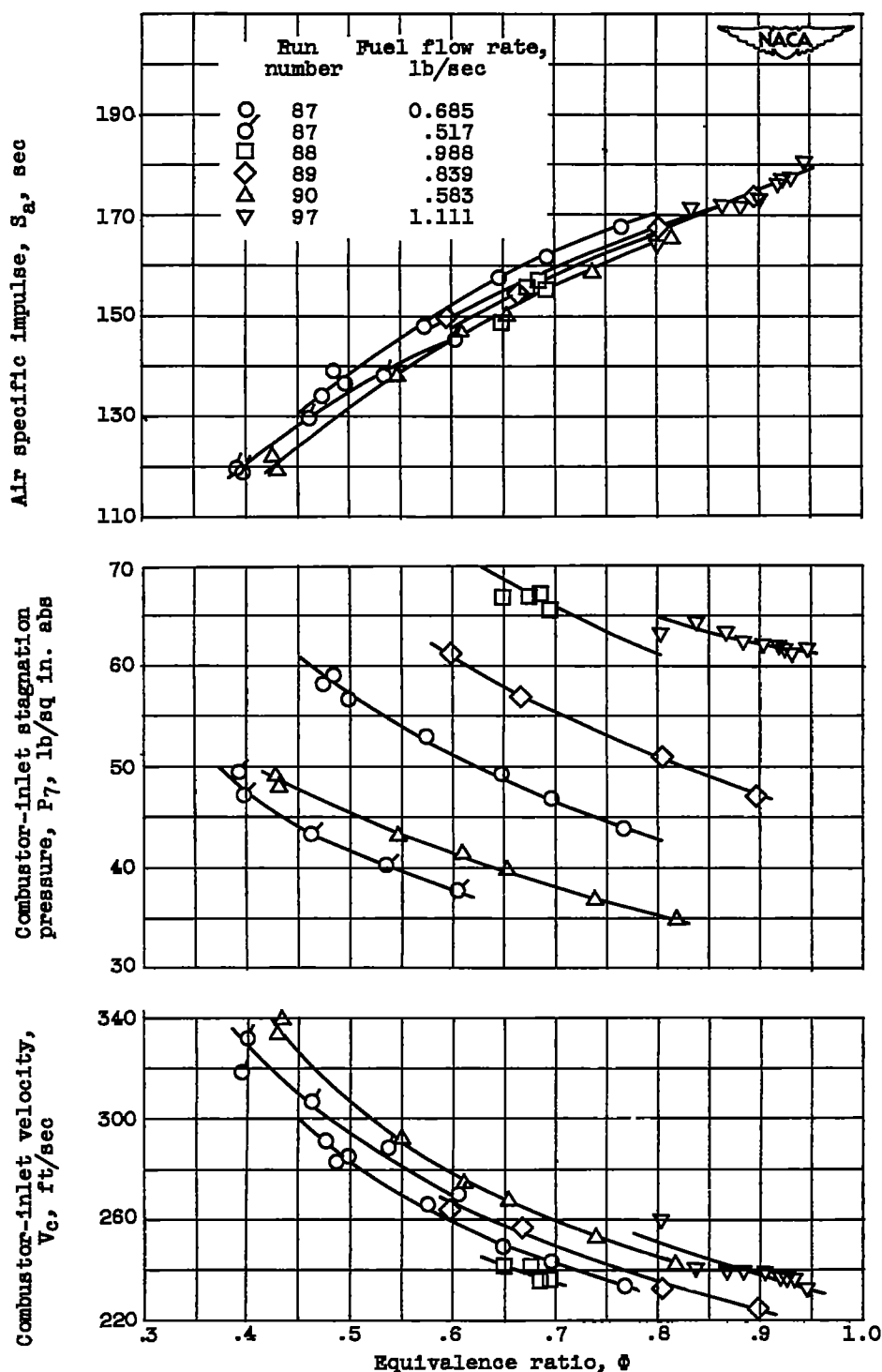


Figure 8. - Effect of equivalence ratio on air specific impulse, combustor velocity, and combustor total pressure for slurries containing 50 percent grade C magnesium in MIL-F-5624A grade JP-3 fuel. Flame holder C, 46 percent blocked area; fuel injector E; nozzle diameter, 6 inches.



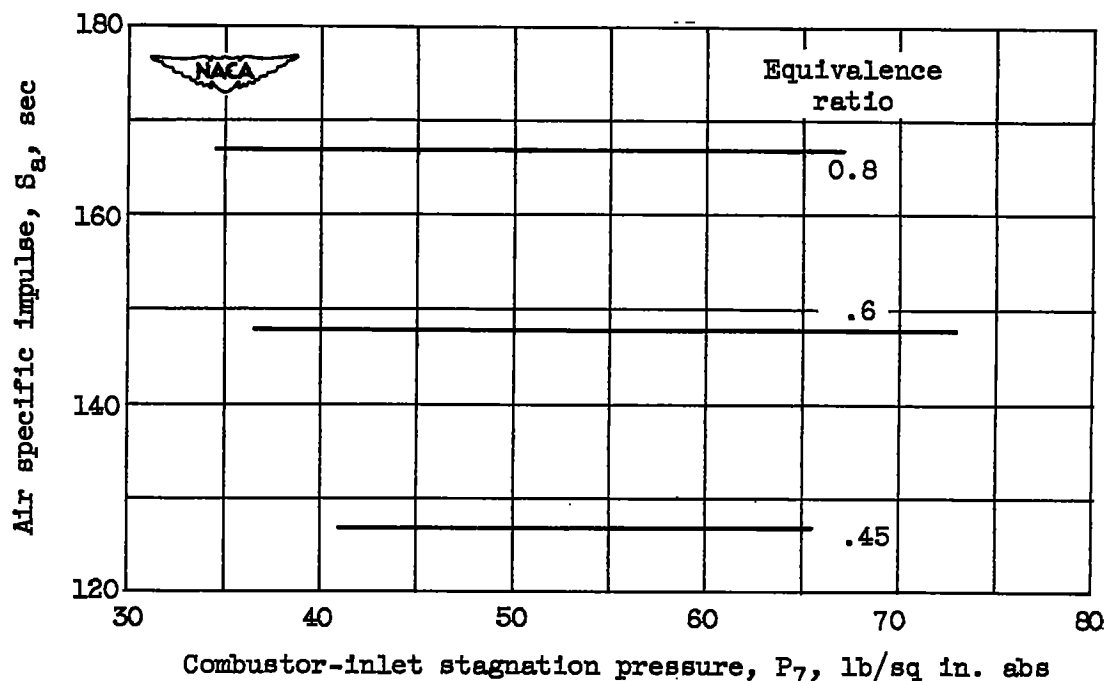


Figure 9. - Effect of combustor pressure on air specific impulse for slurries containing 50 percent grade C magnesium in MIL-F-5624A grade JP-3 fuel. Flame holder C, 46 percent blocked area; fuel injector E; nozzle diameter, 6 inches.

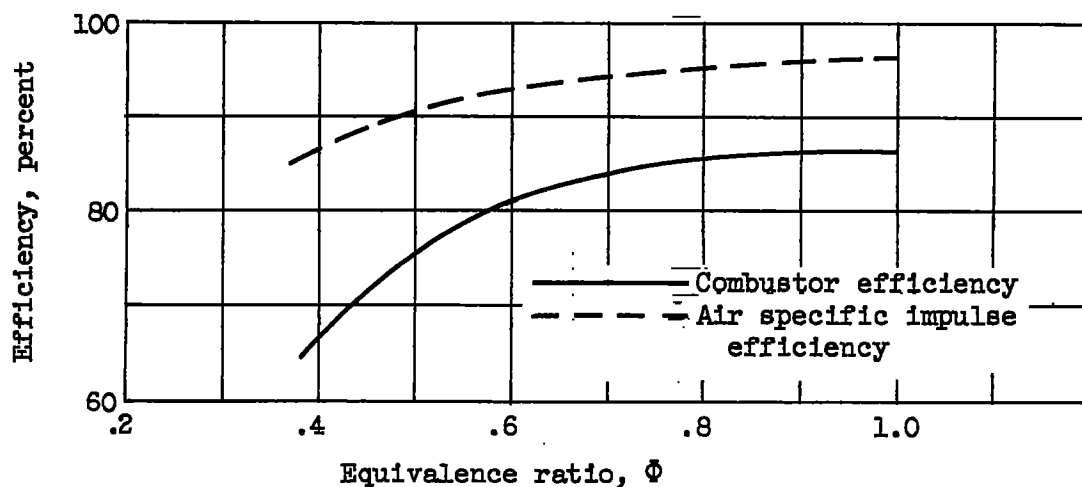


Figure 10. - Combustor and impulse efficiencies for slurries of 50 percent grade C magnesium in MIL-F-5624A grade JP-3 fuel. Flame holder C, 46 percent blocked area; fuel injector E; nozzle diameter, 6 inches.

CI-6 2755

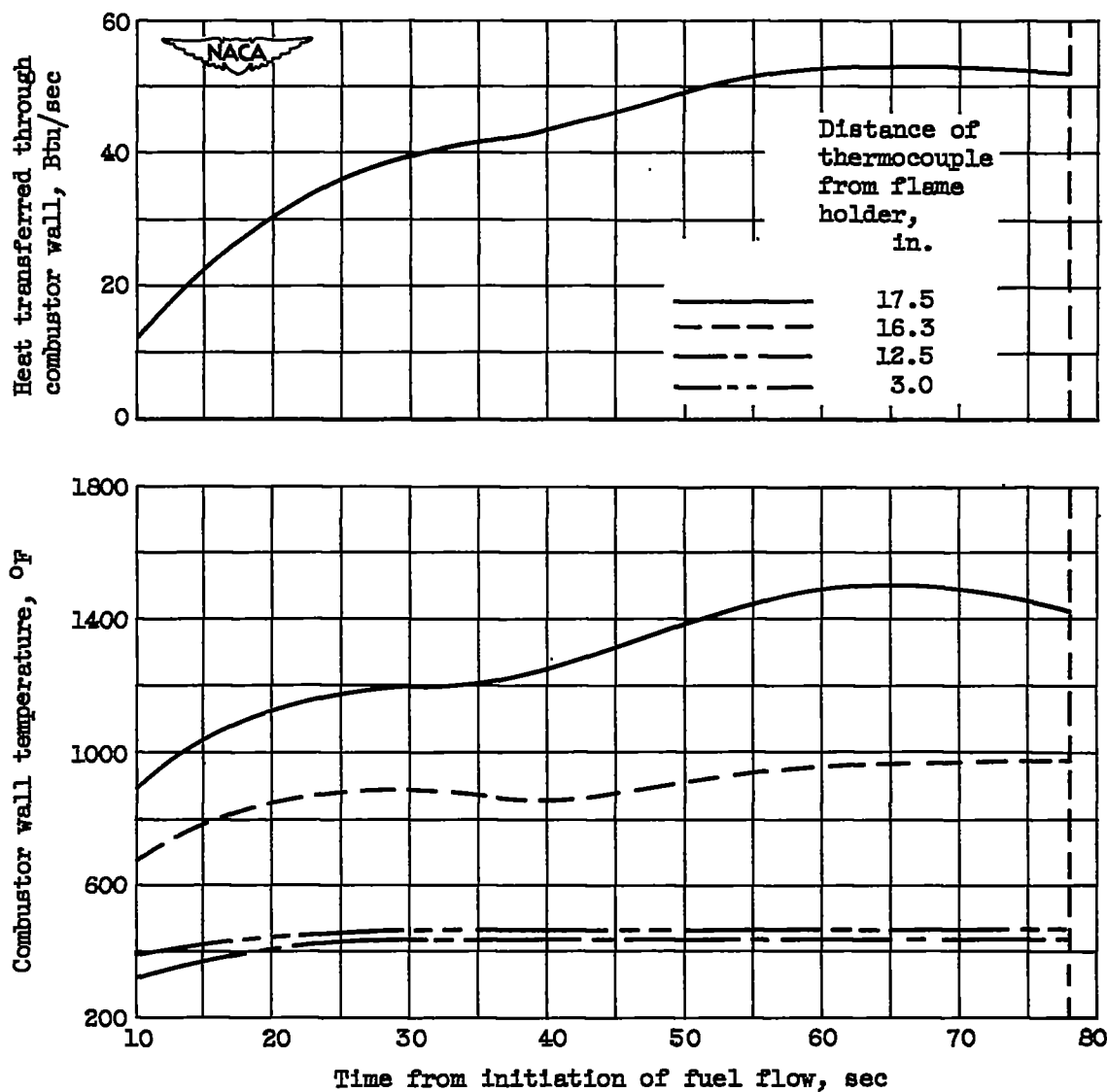


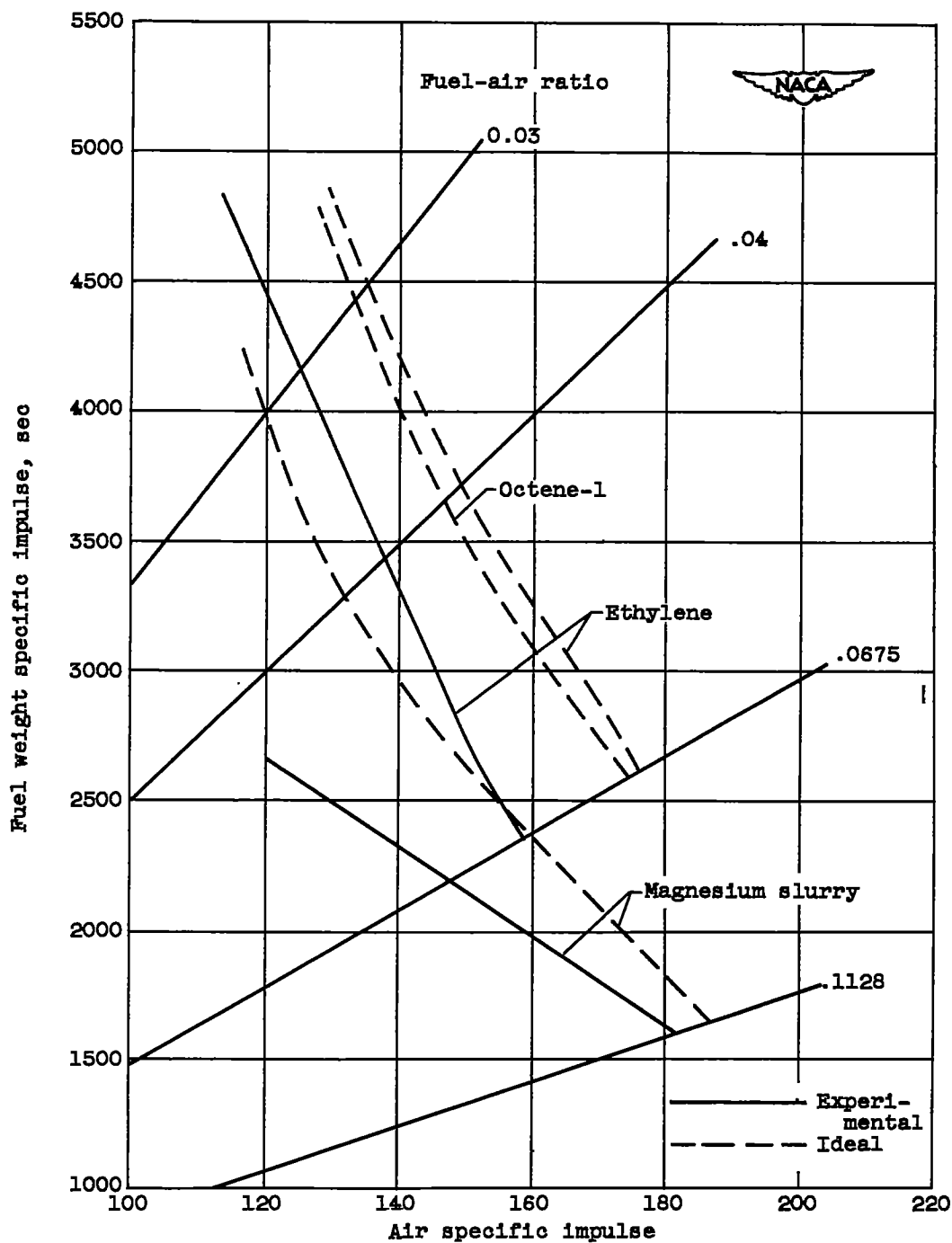
Figure 11. - Combustor wall temperatures and heat transfer rate obtained during run 97 for a slurry consisting of 50 percent grade C magnesium in MIL-F-5624A grade JP-3 fuel. Flame holder C, 46 percent blocked area; fuel injector E; nozzle diameter, 6 inches. Equivalence ratio, 0.836 to 0.947; air flow, 11.78 to 10.40 pounds per second.



(a) After run 87.

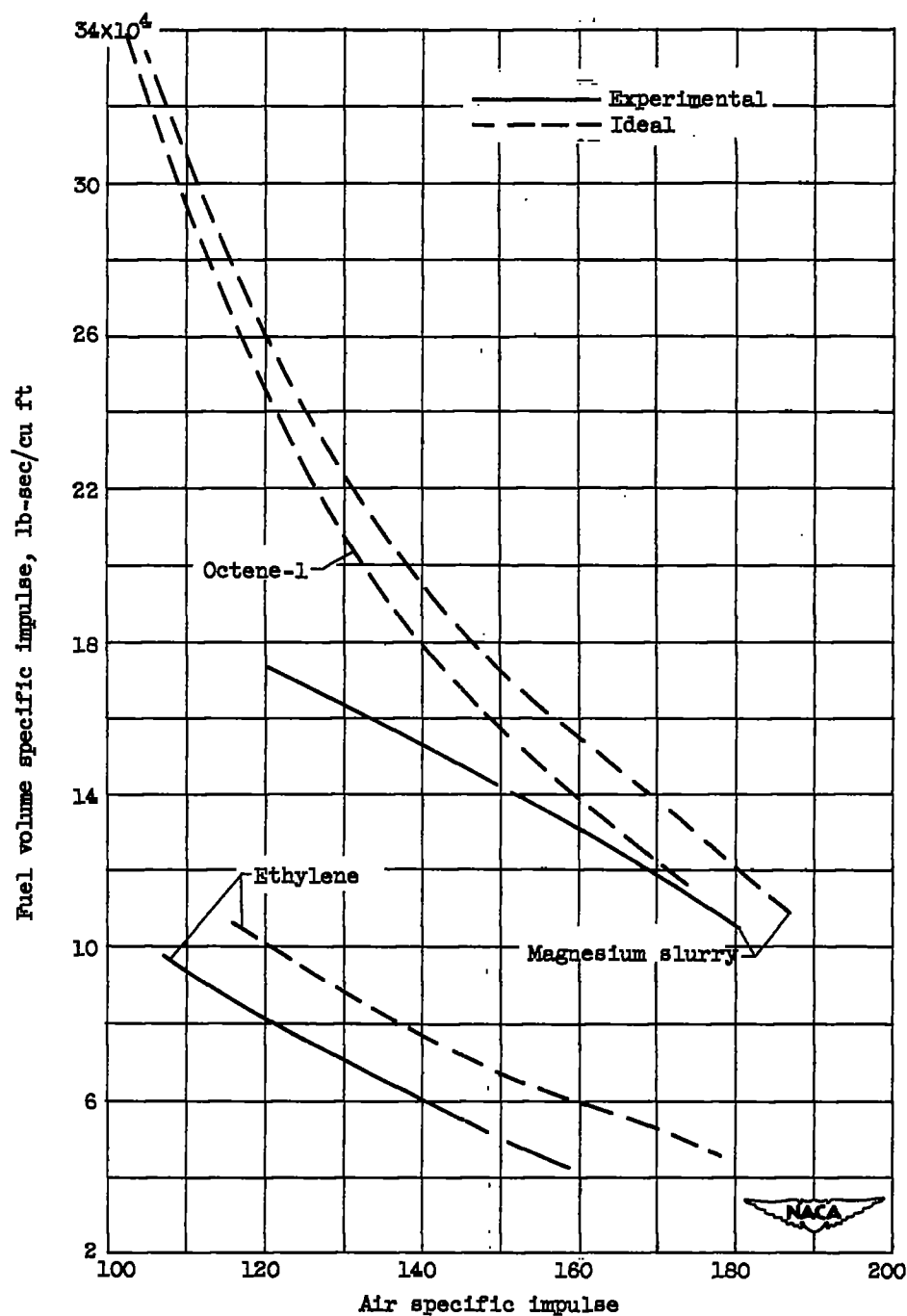
(b) Before run 87.

Figure 12. - Photographs of flame holder.



(a) Fuel weight specific impulse.

Figure 13. - Fuel specific impulse as function of air specific impulse for three fuels. Combustor-inlet stagnation temperature, 350° F; sonic discharge of exhaust products. Experimental slurry data obtained from figure 5 and experimental ethylene data obtained from reference 4.

~~CONFIDENTIAL~~

(b) Fuel volume specific impulse.

Figure 13. - Concluded. Fuel specific impulse as function of air specific impulse for three fuels. Combustor-inlet stagnation temperature,  $350^{\circ}$  F; sonic discharge of exhaust products. Experimental slurry data obtained from figure 5 and experimental ethylene data obtained from reference 4.

~~CONFIDENTIAL~~

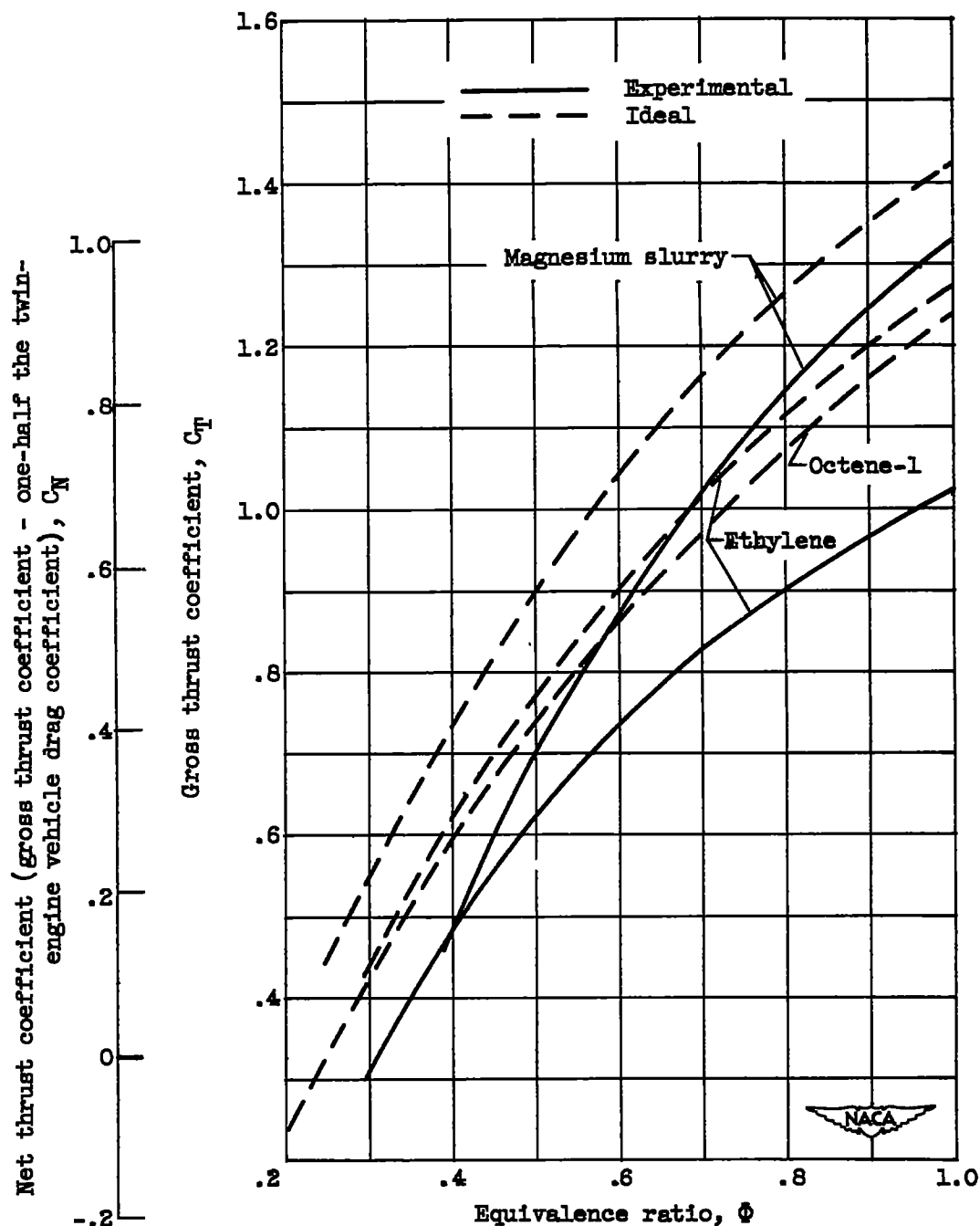


Figure 14. - Effect of equivalence ratio on gross thrust coefficient for two hydrocarbons and a 50 percent magnesium slurry. Simulated free-stream Mach number, 2.3; altitudes above the tropopause. Experimental slurry data obtained from figure 5; experimental ethylene data obtained from reference 4.

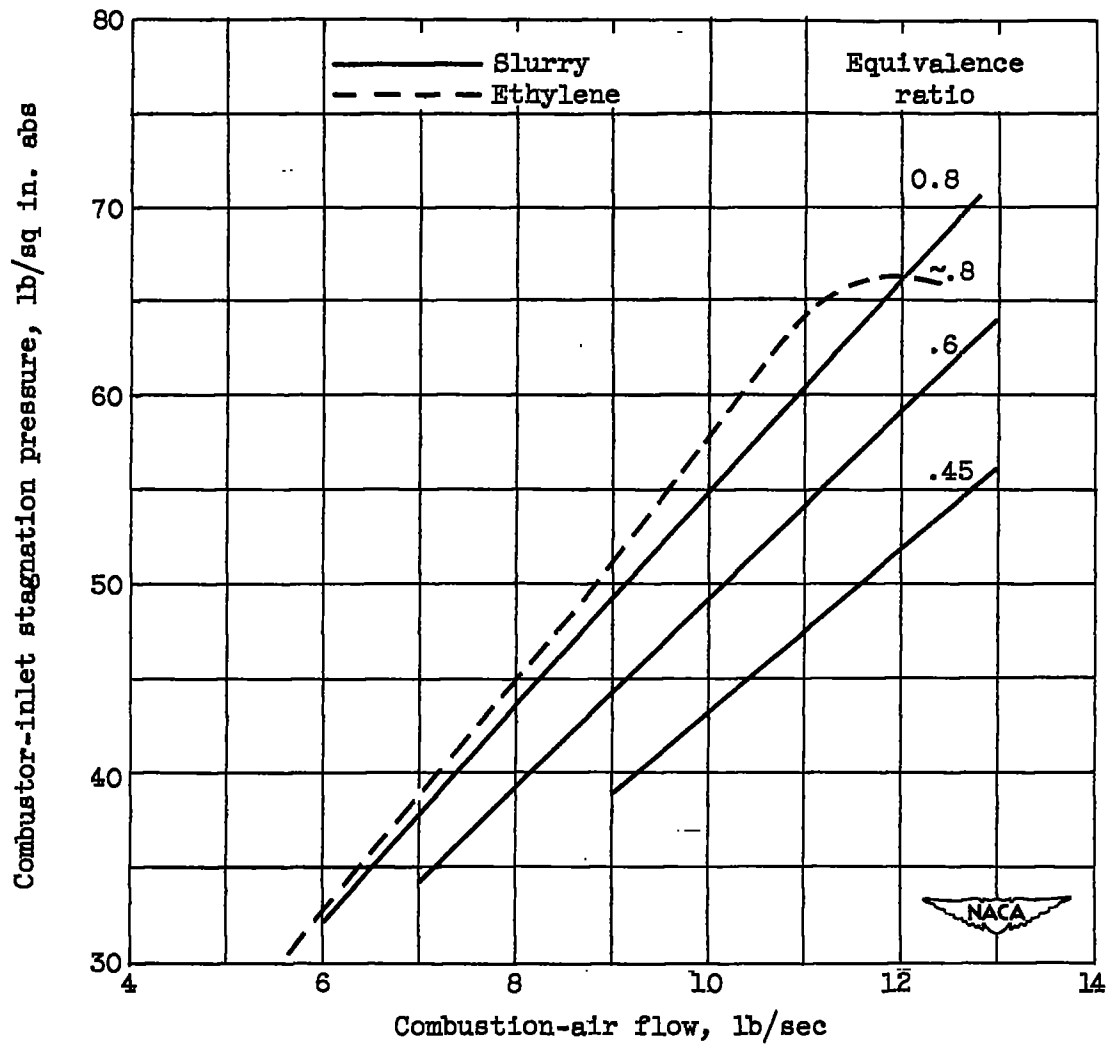
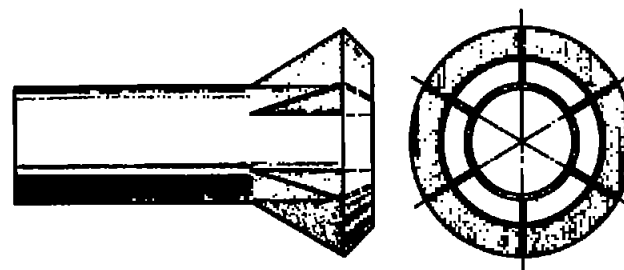


Figure 15. - Comparison of combustor pressure performance of 50 percent grade C magnesium slurry (data from fig. 8) with combustor pressure performance of ethylene in flight (ref. 6). Nozzle throat diameter, 6 inches.



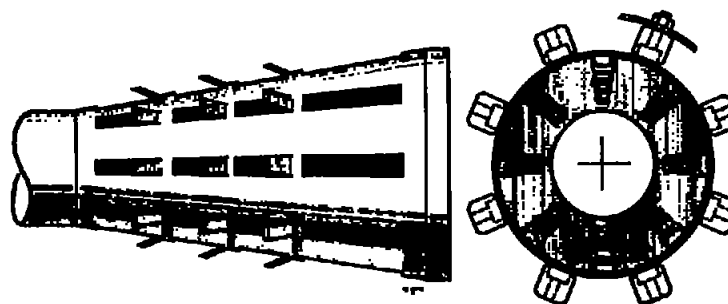
(a) Type A: gutter; 40 percent blocked area.



(b) Type B: funnel; 40 percent blocked area.



(c) Type C: gutter, funnel; 48 percent blocked area.

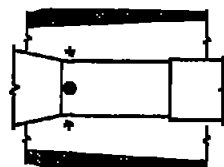


(d) Type D (can).

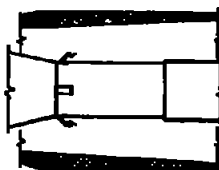
NACA  
RD-2854

Figure 16. - Flame-holder configurations.

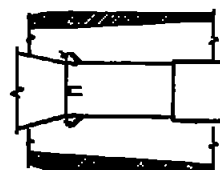




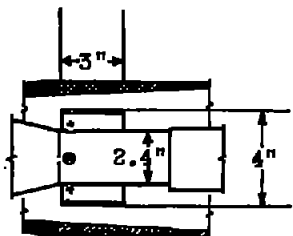
Type A (unobstructed)



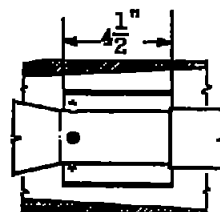
Type B (diagonal rearward-splash)



Type C (diagonal-forward splash)

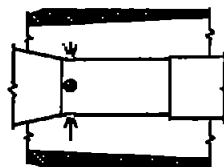


Type D (3-inch sleeve)

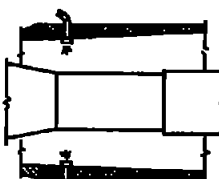


Type E (4.5-inch sleeve)

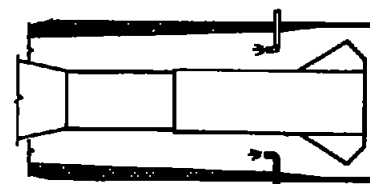
(a) Configurations employing variable-area slots spaced 90° apart.



Type F (radial-outward)



Type G (radial-inward)



Type H (axial)

(b) Configurations employing high-pressure jets spaced 90° apart.



Figure 17. - Fuel-injection configurations.

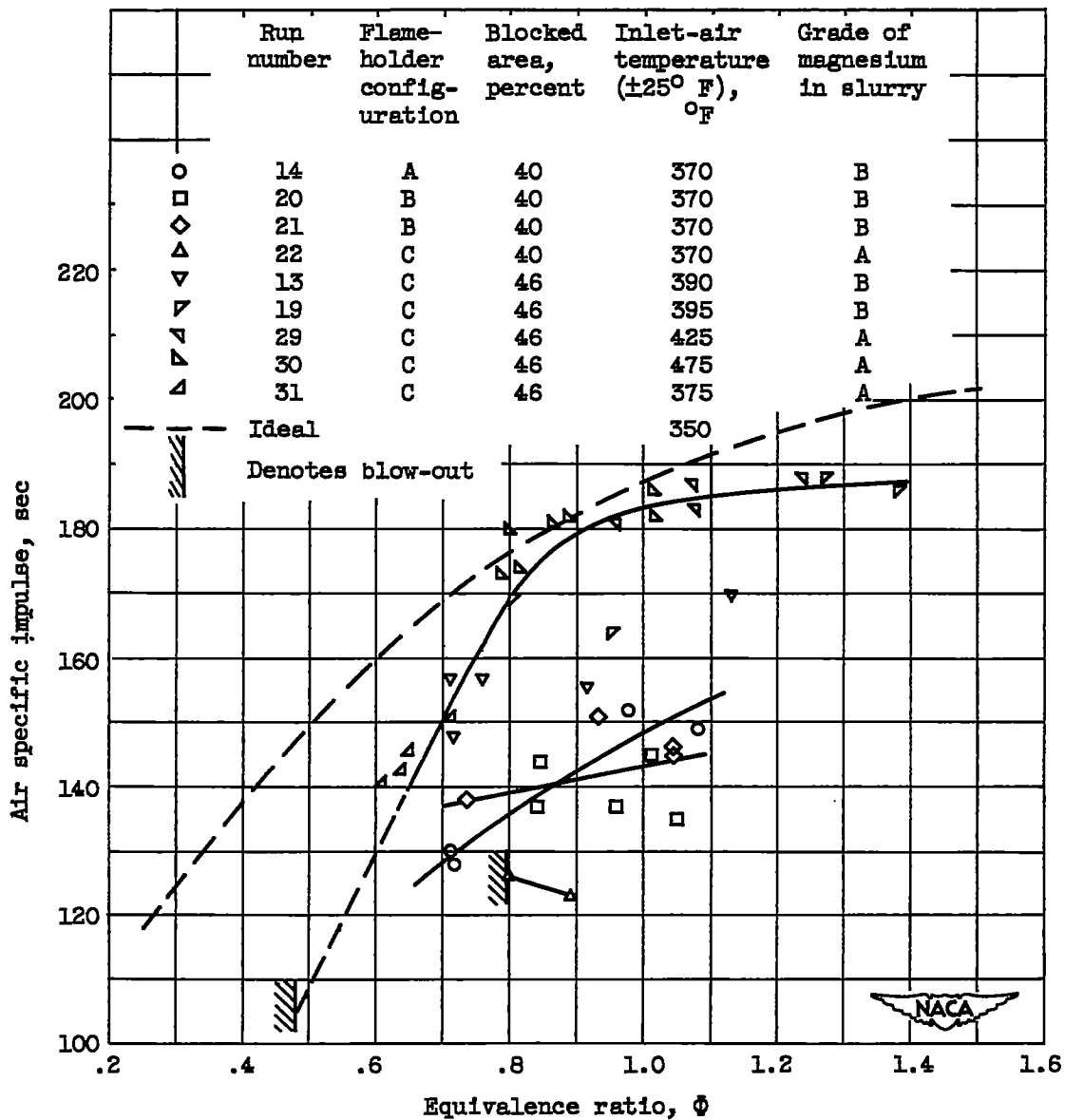


Figure 18. - Effect of several flame-holder configurations on combustion performance. Slurry, 50 percent magnesium in MIL-F-5624A grade JP-3 fuel; fuel injector C; nozzle diameter, 5.66 inches.

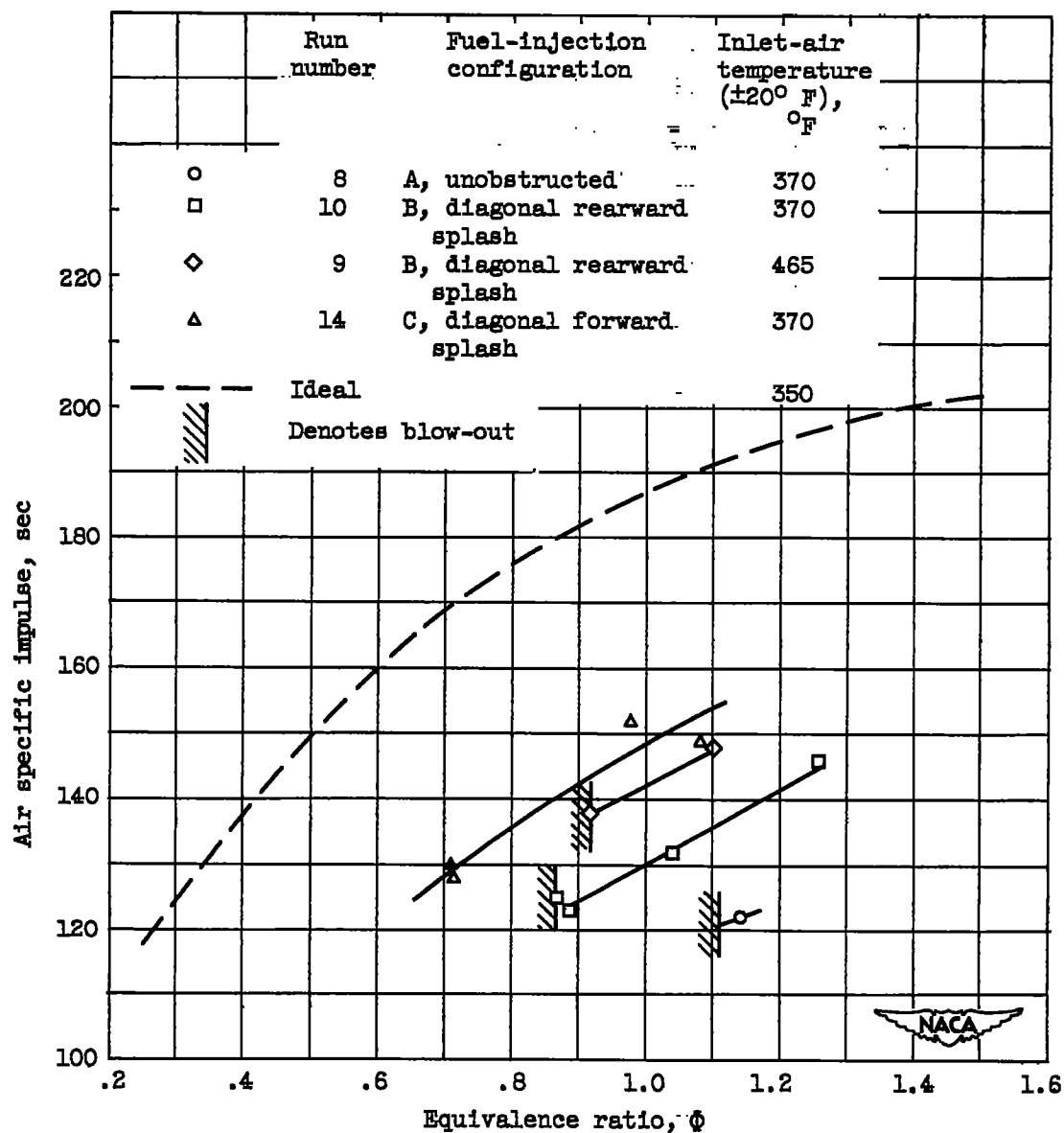


Figure 19. - Effect of diagonal-type splash plates on combustion performance. Slurry, 50 percent grade B magnesium in MIL-F-5624A grade JP-3 fuel; flame holder A; nozzle diameter, 5.66 inches.

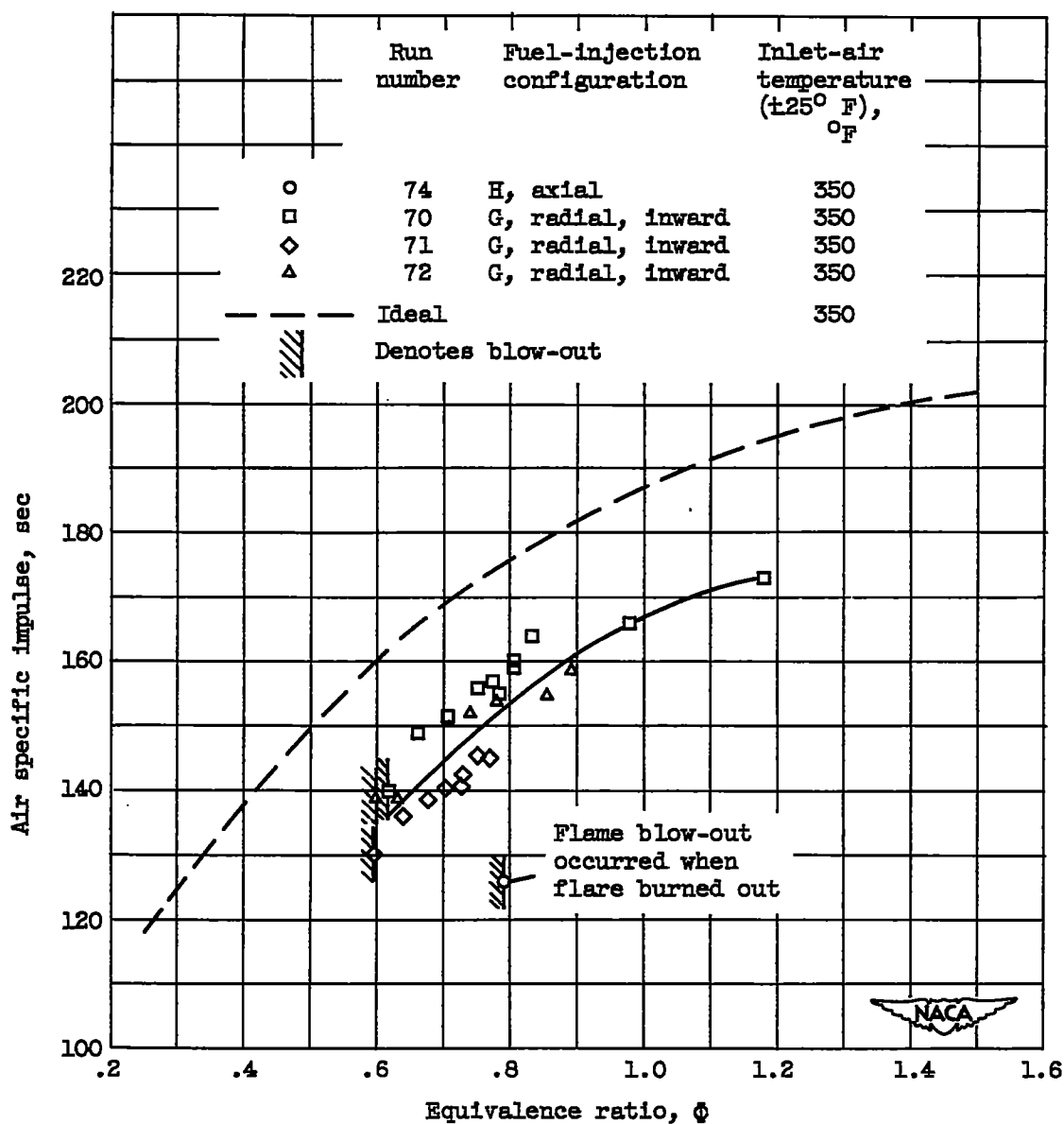


Figure 20. - Effect of location and direction of high-pressure fuel jets on combustion performance. Slurry, 50 percent grade B magnesium in MIL-F-5624A grade JP-3 fuel; flame holder C, 46 percent blocked area; nozzle diameter, 5.66 inches.

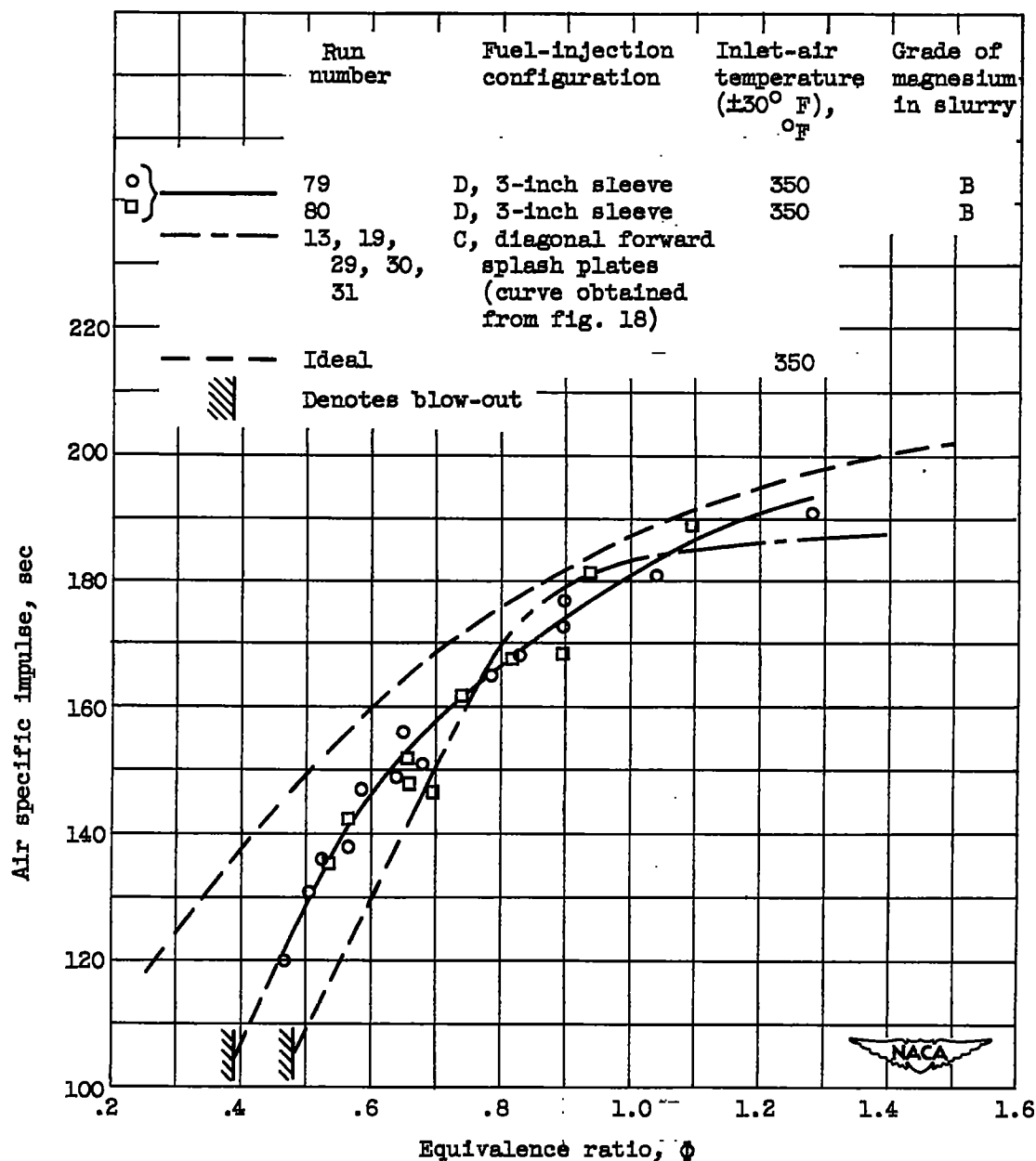


Figure 21. - Effect of fuel distribution control on combustion performance. Slurry, 50 percent magnesium in MIL-F-5624A grade JP-3 fuel; flame holder C; 46 percent blocked area; nozzle diameter, 5.66 inches.

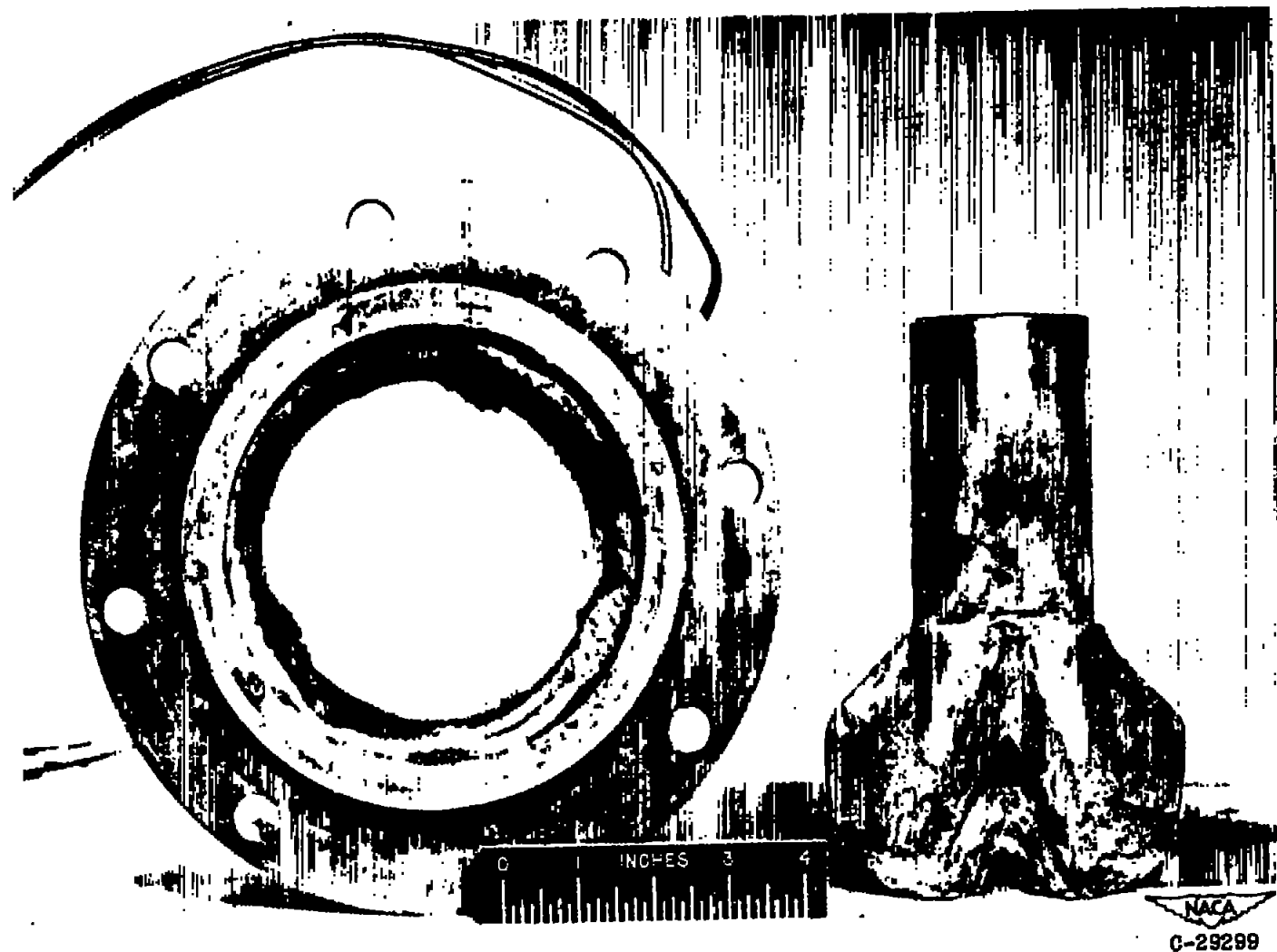
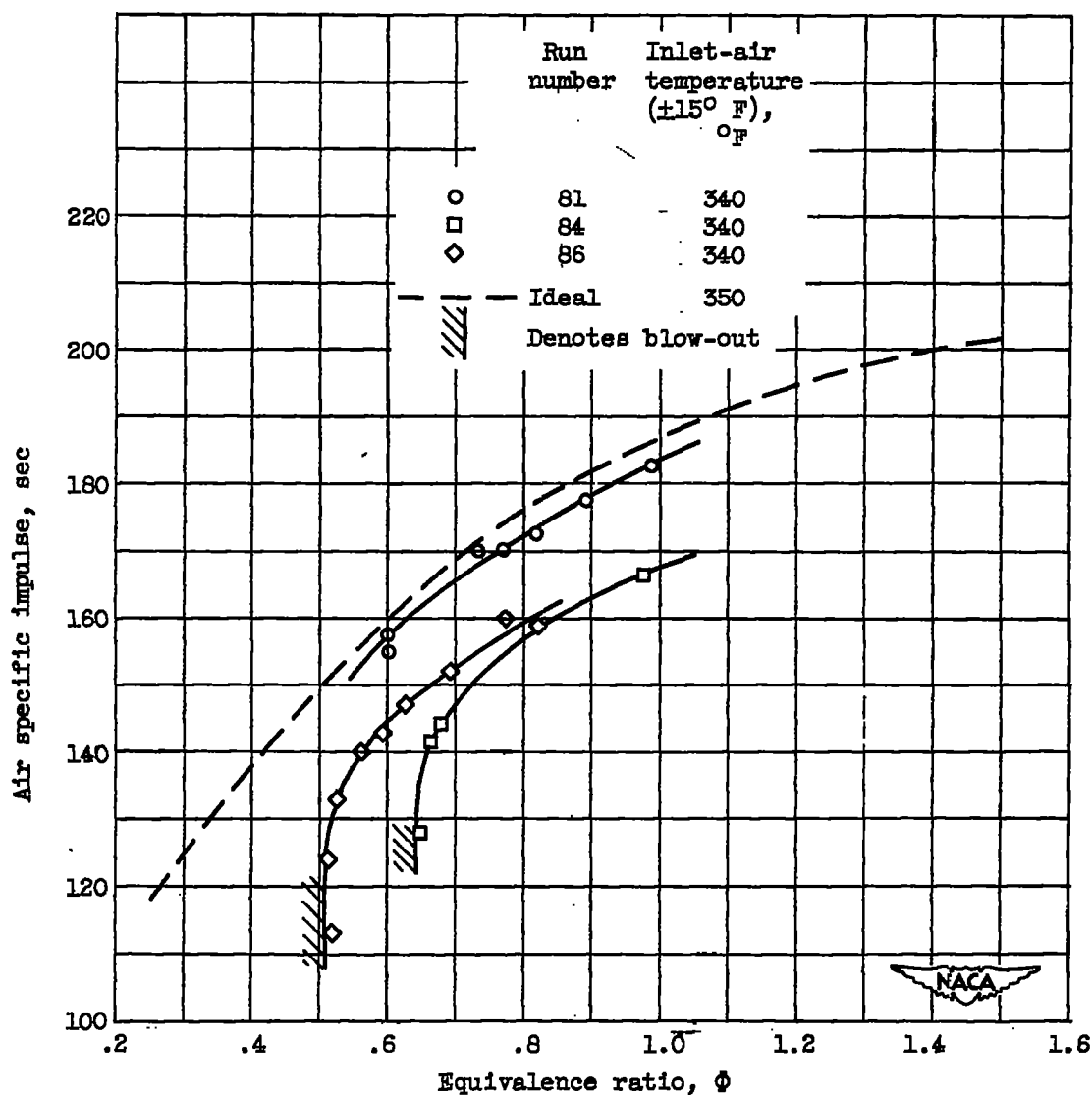
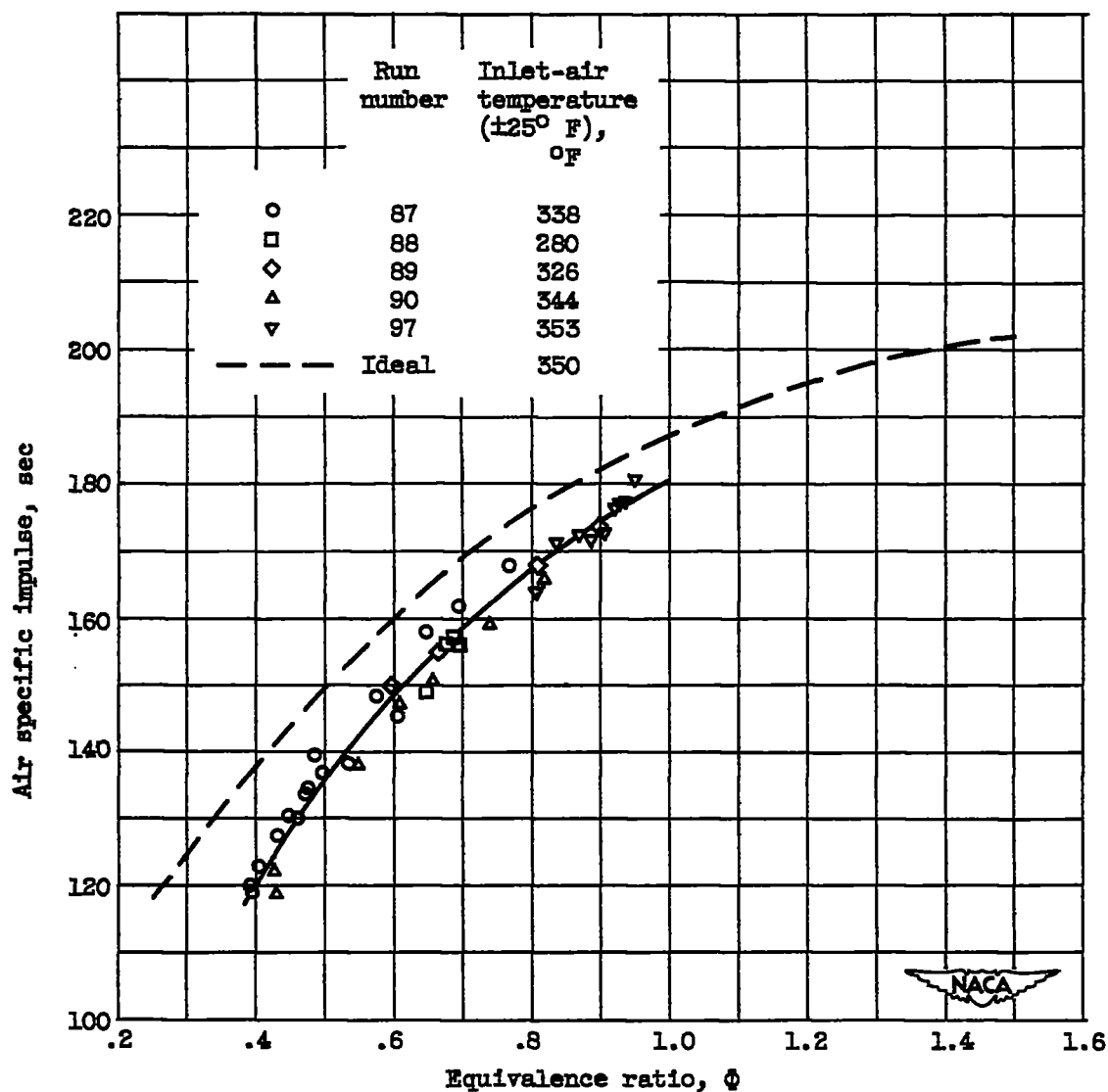


Figure 22. - Combustion deposit obtained in run 79.



(a) Data obtained with 3-inch sleeve, type D injector.

Figure 23. - Effect of injection-control-sleeve length on combustion performance. Slurry, 50 percent grade C magnesium in MIL-F-5624A grade JP-3 fuel; flame holder C, 46 percent blocked area; nozzle diameter, 6.00 inches.



(b) Data obtained with 4.5-inch sleeve, type E injector.

Figure 23. - Concluded. Effect of injection-control-sleeve length on combustion performance. Slurry, 50 percent grade C magnesium in MIL-F-5624A grade JP-3 fuel; flame holder C; 46 percent blocked area; nozzle diameter, 6.00 inches.



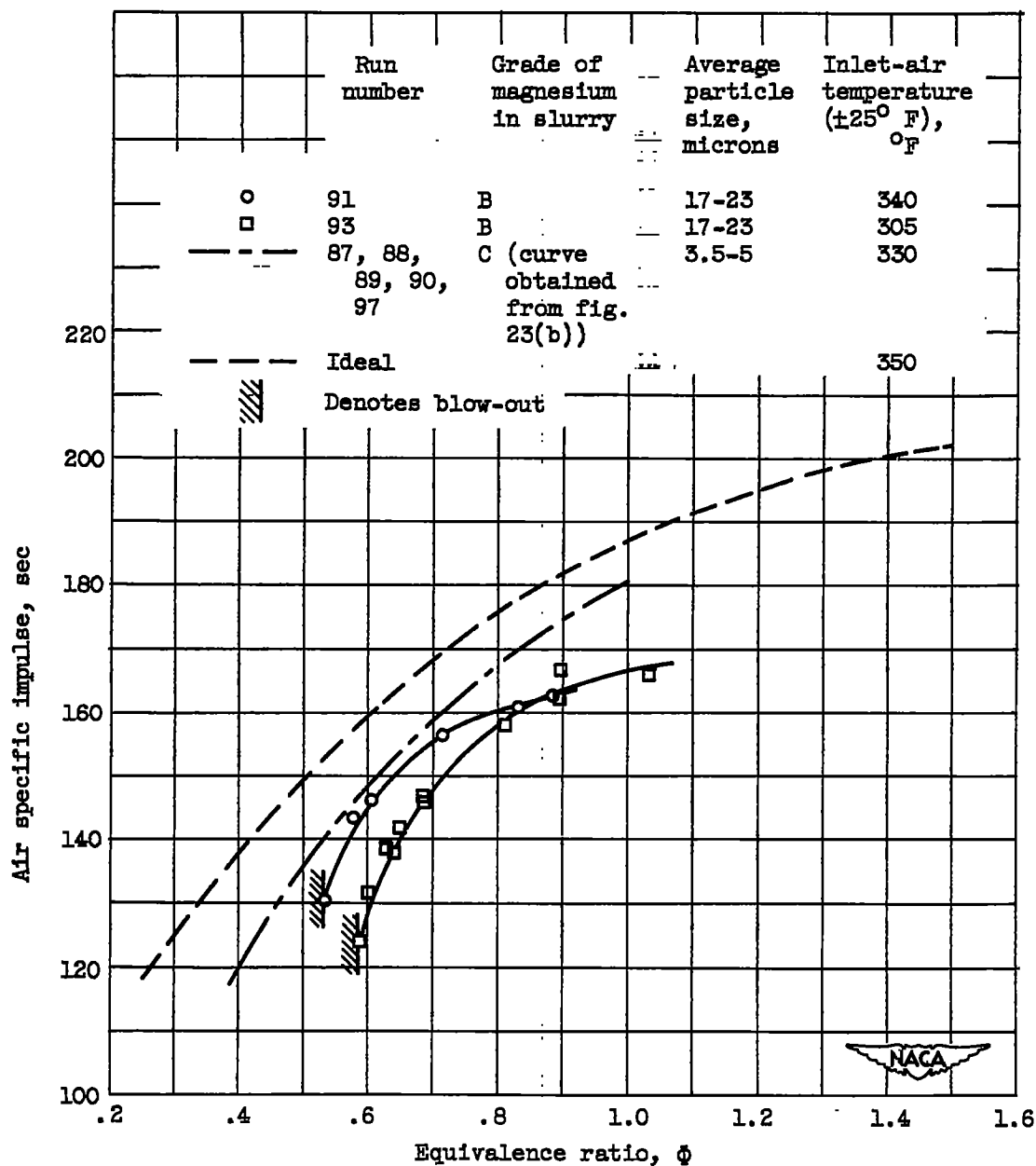


Figure 24. - Effect of magnesium grade on combustion performance of a slurry containing 50 percent magnesium in MIL-F-5624A grade JP-3 fuel. Flame holder C, 46 percent blocked area; fuel injector E; nozzle diameter, 6 inches.

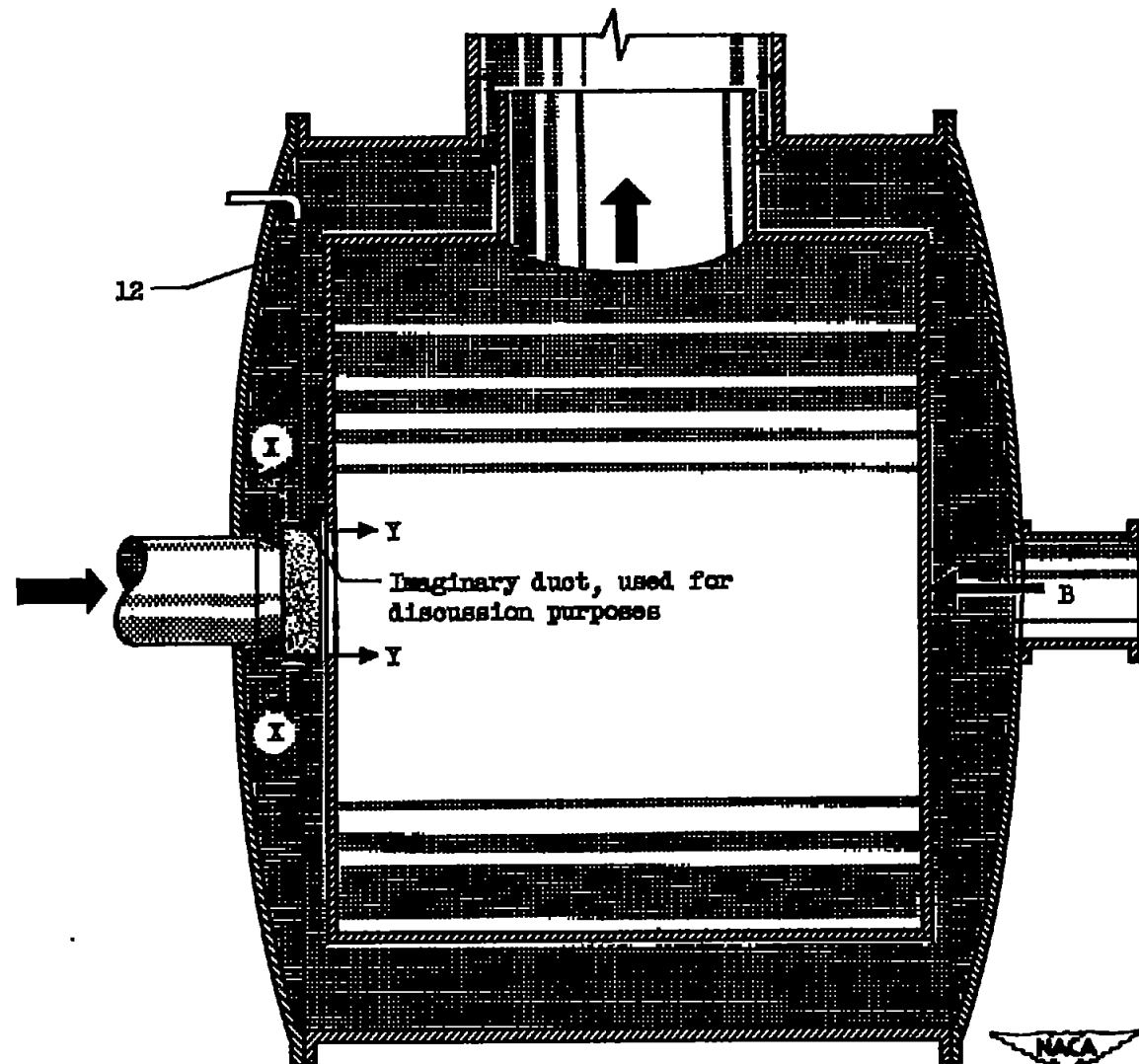


Figure 25. - Sketch of thrust barrel.

NACA  
CD-5071

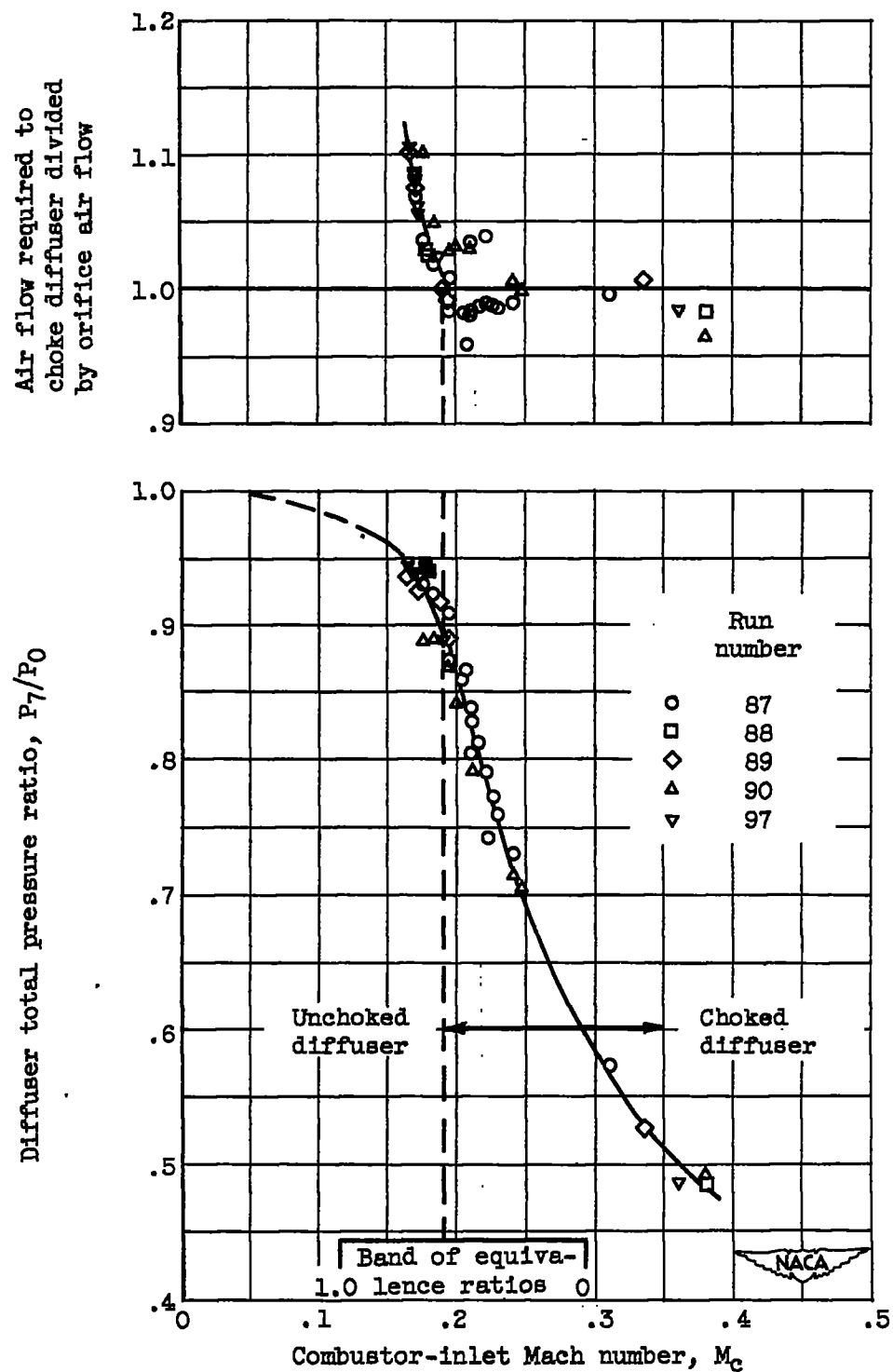


Figure 26. - Effect of combustor-inlet Mach number on pressure ratio and criterion of choke in the diffuser.

2755 •

CI-8 back

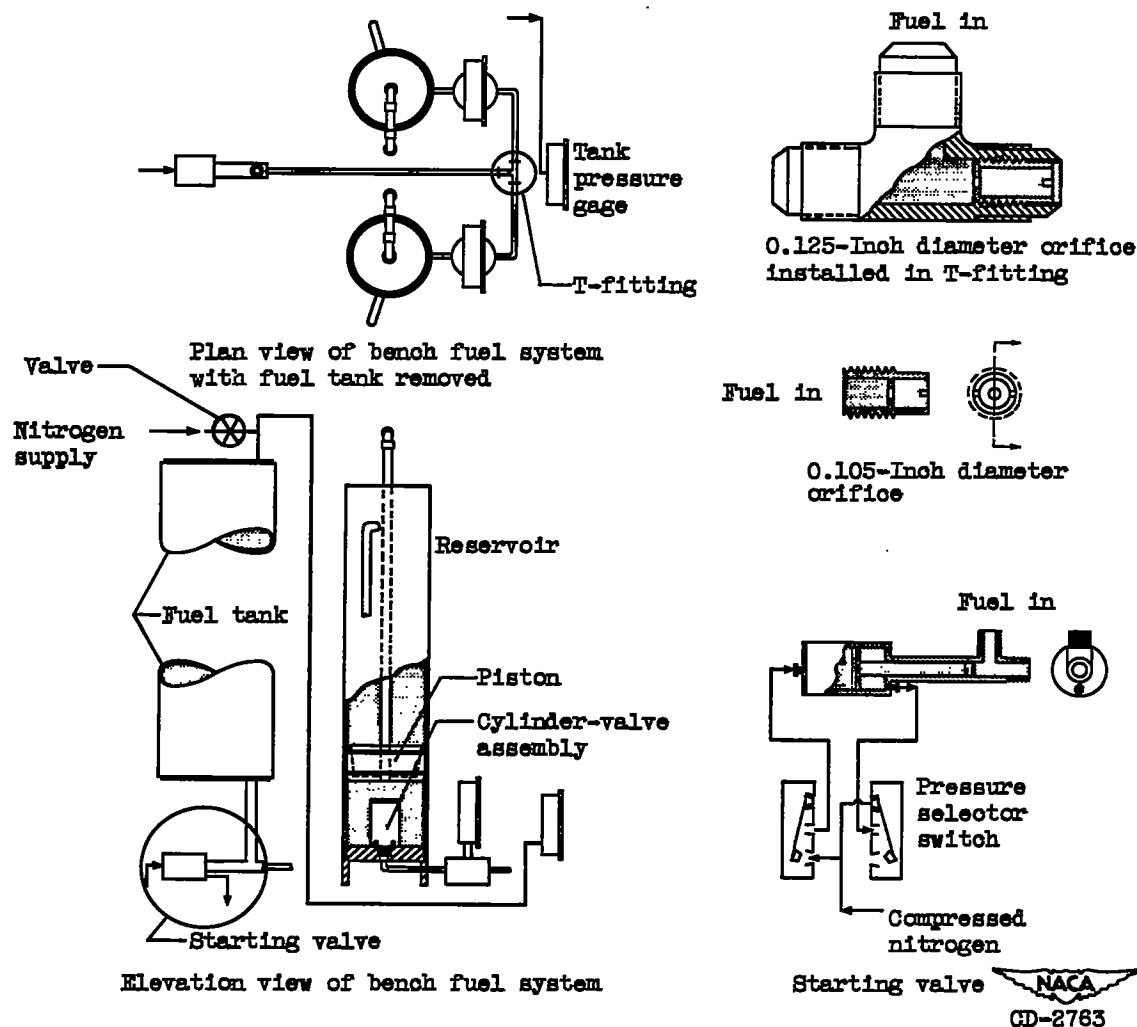


Figure 27. - Diagram of components of bench fuel system.

~~CONFIDENTIAL~~

NACA RM E53E27

2755

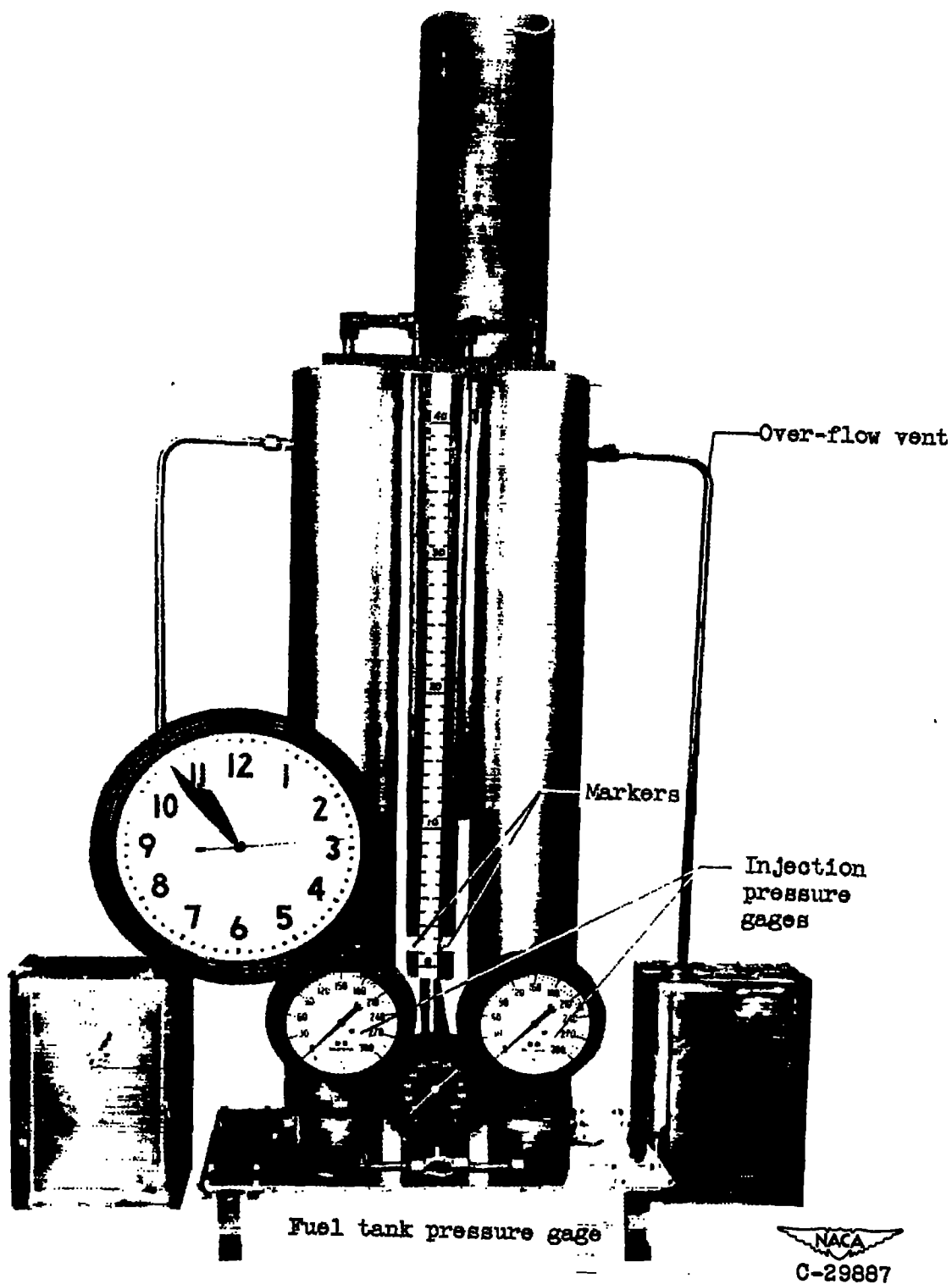
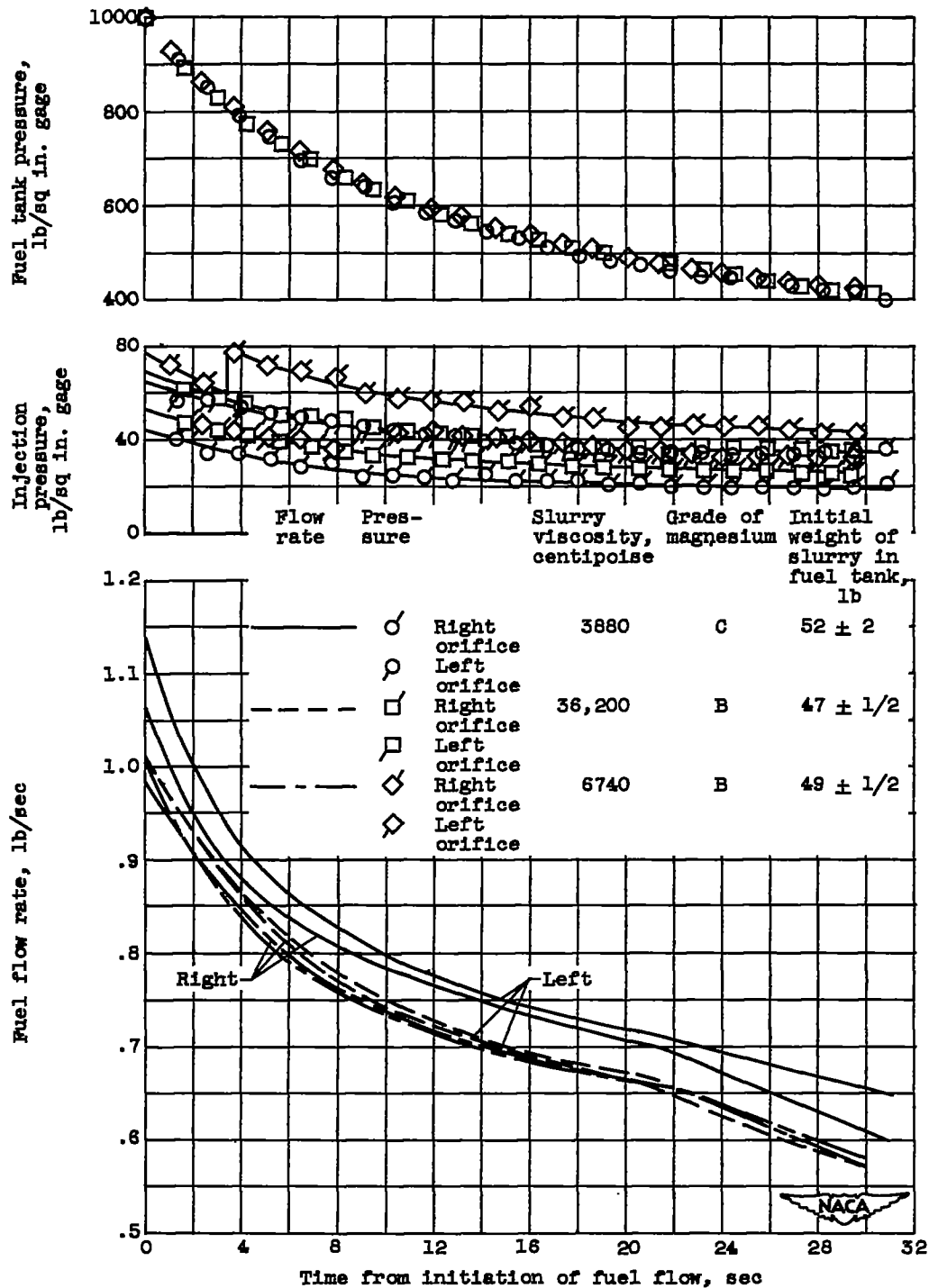


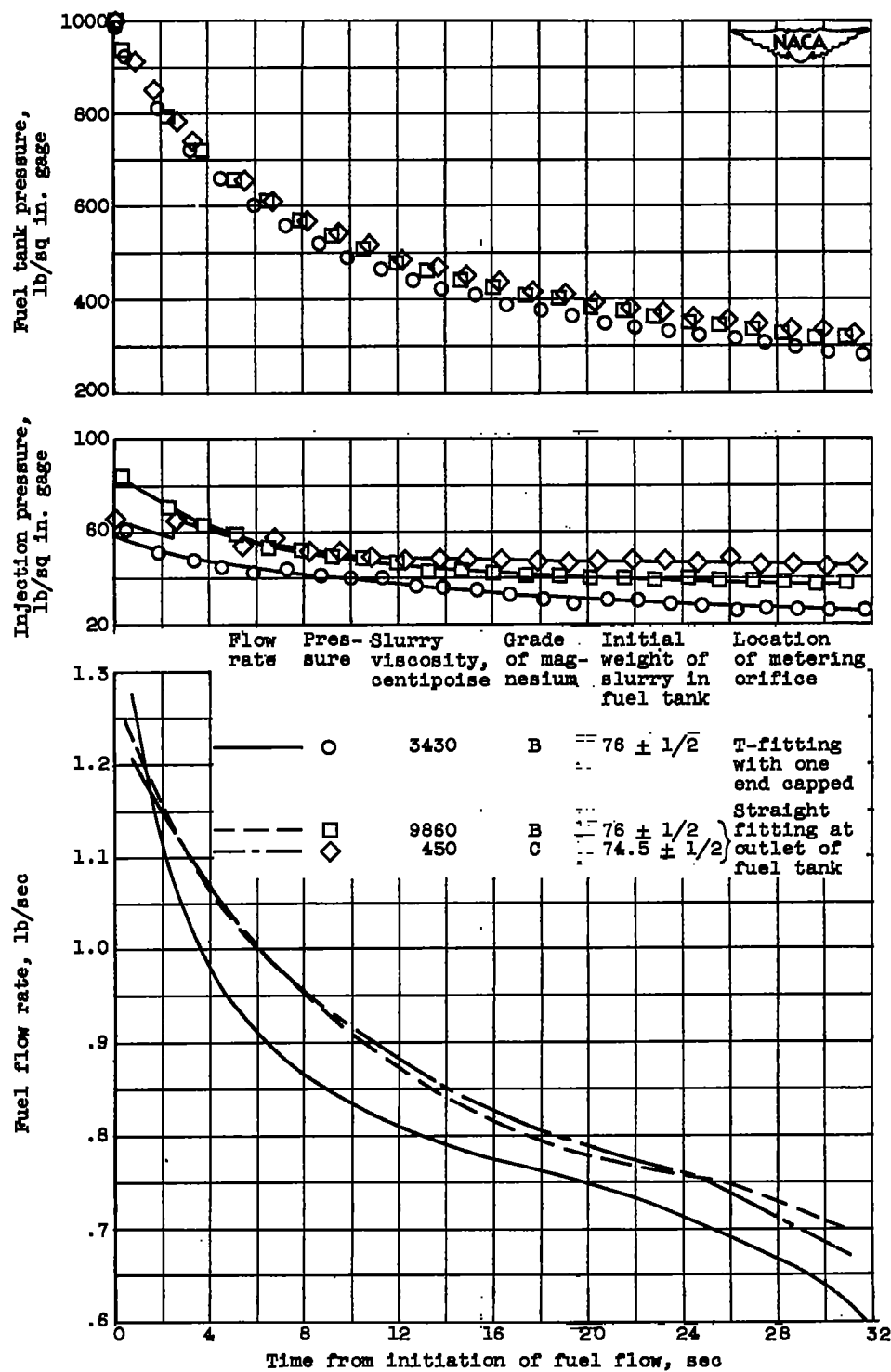
Figure 28. - Photograph of bench fuel system.

~~CONFIDENTIAL~~



(a) Restricted-approach 0.105-inch-diameter orifice mounted in T-fitting.

Figure 29. - Bench fuel system flow rate and pressure data for a 50 percent magnesium slurry.



(b) Unrestricted-approach 0.125-inch-diameter orifice.

Figure 29. - Concluded. Bench fuel system flow rate and pressure data for a 50-percent magnesium slurry.

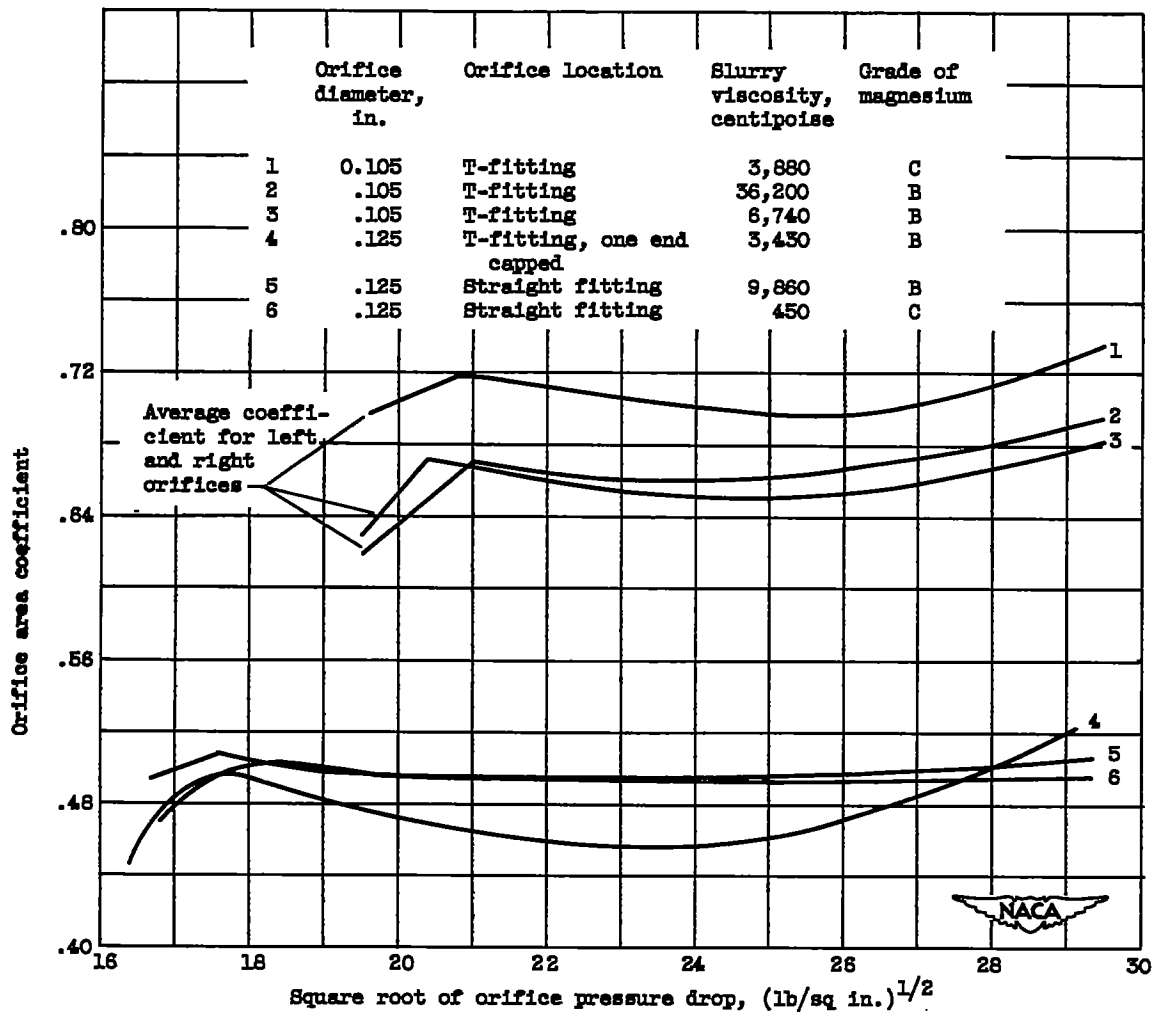


Figure 30. - Orifice area coefficients for two orifices and two orifice locations. 50-Percent magnesium slurry.